



The role of the slab pull force in the late Oligocene to early Miocene extension in the Southern Central Andes (27°–46°S): Insights from numerical modeling



Lucas M. Fennell ^{a,*}, Javier Quinteros ^b, Sofia B. Iannelli ^a, Vanesa D. Litvak ^a, Andrés Folguera ^a

^a CONICET - Universidad de Buenos Aires, Instituto de Estudios Andinos Don Pablo Groeber (IDEAN), Buenos Aires 1428, Argentina

^b GFZ Helmholtz Centre Potsdam, Telegrafenberg, 14473 Potsdam, Germany

ARTICLE INFO

Article history:

Received 26 July 2017

Received in revised form

22 December 2017

Accepted 22 December 2017

Available online 1 February 2018

Keywords:

Subduction

Asthenospheric influx

Synextensional deposition

Intra-arc basin

Back-arc basin

Convergence velocity

ABSTRACT

Although extensional deformation plays a significant part of Andean history, the causes behind its driving mechanisms and its impact throughout the geological record remain controversial. Through the aid of numerical modeling of subduction zone dynamics, we were able to reproduce a brief period of intra-arc basin formation that affected the Southern Central Andes (27°–46°S) during late Oligocene and early Miocene times. The results of the model show that, after a period of slow subduction (6–8 cm/yr), the oceanic plate approaches the mantle transition zone at ca. 23 Ma, triggering the slab pull force. The addition of this slab pull force generates a progressive increase in convergence velocity (reaching ~20 cm/yr) and the retreat of the trench hinge away from the upper plate, resulting in the steepening of the slab. Effects observed in the upper plate are the formation of a basin located 200–300 km east of the trench and an asthenospheric influx beneath an 800 km wide zone east of the oceanic and continental plate's boundary. A series of parameters extracted from our model, such as the basin depth and the stretching factor, indicate that crustal stretching, basin formation, convergence velocity and asthenospheric influx would have reached their climax approximately at 20 Ma. These results are in good correlation with the convergence rate obtained through plate reconstructions and the geological record along the Southern Central Andes, where a series of extensional intra-arc basins were created and mantle derived magmatic processes affected a wide area ranging between the present fore-arc and retroarc areas during late Oligocene to early Miocene times. However, differences in extension magnitude, magma composition and basin fill depositional environment are observed, indicating that the impact of the slab pull force was stronger towards the southern basins. Possible causes that could explain these differences are variations in crustal thickness before the influence of the slab pull force and the effect of toroidal mantle flow near the southern lateral slab edge. This would indicate that although the main parameter controlling tectonic regime is the absolute motion of the overriding plate, the slab pull force may leave its imprint along the evolution of subduction-type orogens such as the Andes.

© 2018 Elsevier Ltd. All rights reserved.

1. Introduction

The Andes are conceived as being constructed through a series of crustal shortening and thickening stages, product of ongoing subduction since at least Early Jurassic times (Mpodozis and Ramos, 1990; Charrier et al., 2007; Ramos, 2009; DeCelles et al., 2009). However, when analyzed in depth, the history of this subduction-

type orogen shows high complexity, alternating extensional and compressional deformational phases along its evolution (Ramos and Kay, 2006; Folguera and Ramos, 2011; Folguera et al., 2015; Echaurren et al., 2016). The birth of the Andean Cordillera took place during Cretaceous times, associated with the Southern Atlantic Ocean opening and the westward movement of the South American plate (Coney and Evenchick, 1994; Somoza and Zaffarana, 2008). As a consequence, the passage from an extensional regime, related to the break-up of Gondwana, towards a compressional regime occurred along the South American western margin

* Corresponding author.

E-mail address: lucasfennell90@gmail.com (L.M. Fennell).

(Ramos, 2010). Most works have been dedicated to study the building of the Andes through the analysis of their contractional phases, focusing on the onset of deformation, rate of uplift and structural style (e.g., Baby et al., 1992; Allmendinger et al., 1997; Kley et al., 1999; Ramos et al., 2004; Blisniuk et al., 2005; Mora et al., 2006; Oncken et al., 2006; Strecker et al., 2007; Garzione et al., 2008; McQuarrie et al., 2008; Giambiagi et al., 2012; Hoke et al., 2014; Horton and Fuentes, 2016). Nevertheless, extensional deformation has also been present in the Andes during their history, although the processes responsible for it remain unclear (e.g., Mpodozis and Allmendinger, 1993; Hervé et al., 1995; Suárez and Emparán, 1995; Charrier et al., 1996; Godoy et al., 1999; Muñoz et al., 2000; Jordan et al., 2001; McNulty and Farber, 2002; Giovanni et al., 2010; Noury et al., 2017).

After their initial structuration, the evolution of the Andes shows differences along strike, associated with local events controlling deformational processes, resulting in the present segmentation of the margin (Gansser, 1973; Ramos, 1999). During the Paleogene, while the central section of the Central Andes (14° – 27° S) experienced an important compressional stage (Horton, 2005; McQuarrie et al., 2005; Gillis et al., 2006; O'Driscoll et al., 2012), the southern sector (27° – 46° S) was experiencing a stage of apparent tectonic quiescence (Ramos and Kay, 2006; Horton and Fuentes, 2016). Plate reconstructions show that differences in the tectonic regime along the margin were influenced by the geodynamic context, dominated by slow (~6 cm/yr) and oblique (40° – 50°) convergence during these times (Fig. 1) (Pardo-Casas and Molnar, 1987; Somoza and Ghidella, 2012; Müller et al., 2016). Oblique subduction in the Southern Central Andes (27° – 46° S) was represented by a neutral tectonic regime, evidenced by poorly evolved arc magmatism (Iannelli et al., 2017; Fernández Paz et al., 2017a) and sparse evidence of transpression and extension (Charrier et al., 2002, 2015; Cobbold and Rosello, 2003) associated with limited subsidence in the foreland, averaging only 25 m/Myr (Horton et al., 2016). The geodynamic setting changed towards the beginning of the Neogene, when subduction became nearly orthogonal (15° – 5°) and convergence rate increased to ~15 cm/yr (Fig. 1) (Pardo-Casas and Molnar, 1987; James and Sacks, 1999; Somoza and Ghidella, 2012; Müller et al., 2016). Also, at about the same time (ca. 23 Ma), the splitting of the Farallon plate gave birth to the Nazca and Cocos plates (Fig. 1) (Lonsdale, 2005). Since then, convergence rate has decreased continuously during the ongoing uplift of the Andes, until reaching the current velocity of ca. 8 cm/yr (Fig. 1) (Gripp and Gordon, 2002; Somoza and Ghidella, 2012).

Over the last decades, numerical models started to test different parameters involved in subduction processes, and many used a comparison with real case scenarios from the Andes in order to validate their results (e.g., van Hunen et al., 2002; Sobolev and Babeyko, 2005; Gerbault et al., 2009; van Dinther et al., 2010; Capitanio et al., 2011; Gibert et al., 2012; Manea et al., 2012, 2017; Quinteros and Sobolev, 2013; Cerpa et al., 2014, 2015). Nevertheless, since most of them are focused on contractional processes, extensional deformation has been less assessed (Schellart, 2008; Schellart and Moresi, 2013).

The subduction parameters that govern back-arc deformation have been analyzed, linking them to present and past tectonic regimes along the Andes (Marrett and Strecker, 2000; van Hunen et al., 2002, 2004; Sobolev and Babeyko, 2005; Heuret and Lallemand, 2005; Oncken et al., 2006; Schellart, 2008; Espurt et al., 2008; Gerbault et al., 2009; Ramos, 2010). These works show that a first-order control is the absolute motion of the overriding plate, which produces either the retreat of the trench hinge away from the upper plate, generating widespread extension, or the advance of the upper plate towards the trench, generating strong coupling and compression. The role of an age-dependent

slab rollback seems to be minor with respect to these forces, since the influence of the slab pull force in back-arc deformation along present subduction settings is not straightforward (Royden, 1993). However, this effect could be considered as a second-order parameter which, among others such as oceanic ridge collisions, changes in the slab dip, dynamic mantle flow and rheological variations in both the down-going and upper plates, can induce motion of the trench hinge and local variations between contractional or tensile regimes (Heuret and Lallemand, 2005; Schellart, 2008; Gerbault et al., 2009; Ramos, 2010).

Nevertheless, although the absolute velocity of South America did not suffer any major change during the Paleogene to Neogene transition (Somoza and Ghidella, 2012; Maloney et al., 2013; Colli et al., 2014; Müller et al., 2016), the southern Central Andes (27° – 46° S) experienced an extensional regime between late Oligocene and early Miocene times (Suárez and Emparán, 1995; Hervé et al., 1995; Charrier et al., 1996; Godoy et al., 1999). The steepening of the slab angle (Muñoz et al., 2000; Folguera and Ramos, 2011; Encinas et al., 2016) and the increase in the convergence rate indicating diminished plate coupling (Jordan et al., 2001; Horton and Fuentes, 2016) are predominant among the proposed causes, which indicates that geodynamic processes would be the best fitting explanation for this regional scale event.

This work aims to understand, through numerical modeling, the causes behind the extensional regime that occurred in the Southern Central Andes between late Oligocene and early Miocene times. Based on the Andean subduction reference model from Quinteros and Sobolev (2013), this paper analyzes the link between the slab pull force, stretching of the crust, increase in convergence rate and the inception of extensional intra-arc basins and associated magmatism between 27° and 46° S. These results indicate that the slab pull force may dominate during brief periods of time, leaving its imprint in the geological record.

2. Geological setting

Recent works have described and constrained an extensional deformation phase between the late Oligocene and the early Miocene, showing numerous evidences of crustal stretching that generated a series of extensional intra-arc basins along the Andes between 27° S and 46° S (Fig. 2) (Jordan et al., 2001; Charrier et al., 2002; Burns et al., 2006; Folguera et al., 2010; Garcia Morabito and Ramos, 2012; Orts et al., 2012; Ramos et al., 2014; Bechis et al., 2014; Winocur et al., 2015; Encinas et al., 2016). Also, this period coincided with voluminous eruptions of mafic and silicic volcanism, whose products are found interbedded in the extensional intra-arc basins sediments and outcropping as a series of magmatic belts and plateaux spread between present fore-arc and retroarc positions (Fig. 2) (Lopez-Escobar and Vergara, 1997; Muñoz et al., 2000; Kay et al., 2005, 2006, 2007; Kay and Copeland, 2006; Litvak et al., 2007, 2015; Dyhr et al., 2013a, 2013b; Encinas et al., 2016).

The geodynamic context of the South American western margin between 27° and 46° S during the extensional regime involved the subduction of the newly formed Nazca oceanic plate, with ages ranging between 40 and 60 Ma (Müller et al., 2016) beneath the South American plate (Fig. 2). This occurred at an almost orthogonal orientation, with Nazca plate moving eastward at rates of ~15 cm/yr and the South American plate overriding westward at ~3 cm/yr (Fig. 2) (Pardo-Casas and Molnar, 1987; Somoza and Ghidella, 2012; Colli et al., 2014).

The late Oligocene to early Miocene extensional regime seemed to have a large impact along the geological record of the Southern Central Andes (27° – 46° S), registering from intra-arc basins with calc-alkaline volcanic infill to the north (Doña Ana basin; Winocur

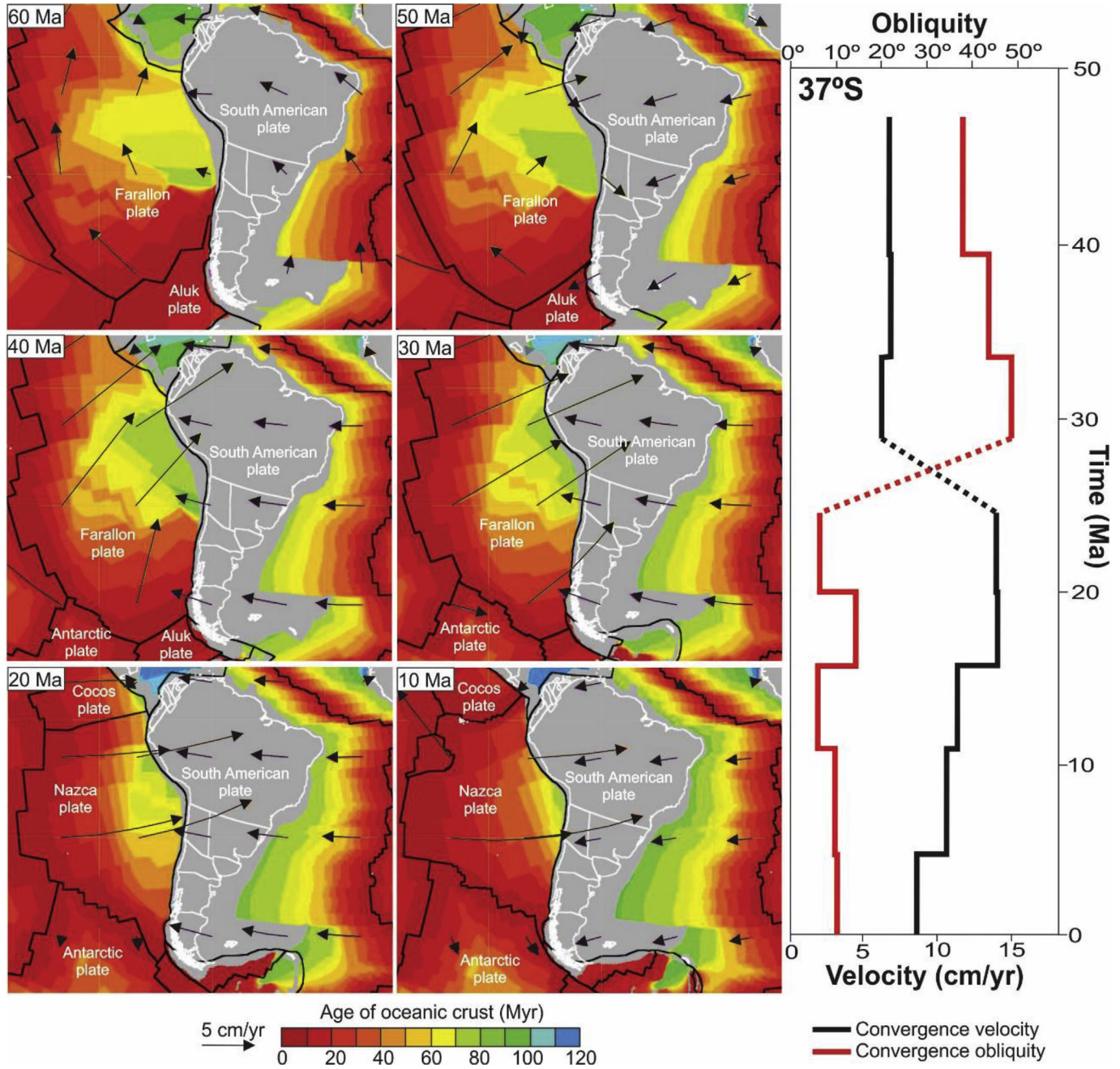


Fig. 1. a) Paleoreconstruction of the convergence history along South America's western margin based on Müller et al. (2016). After a slow and oblique subduction during most of the Paleogene, the beginning of the Neogene coincides with the break-up of the Farallon plate, an increase in convergence rate and a change towards nearly orthogonal subduction (convergence rates and obliquity curves for 37°S are from Somoza and Ghidella, 2012).

et al., 2015), which pass transitionally towards intra-arc basins with mixed tholeiitic volcano-sedimentary infill to the south, where the crust has been hypothesized to have been less than 33 km thick allowing widespread marine transgressions (Traiguén basin, Encinas et al., 2016) (Fig. 2). The geological record of these extensional basins has been studied through outcrops and seismic records, so their areal extent, dynamics of sediment accumulation and basin fill composition are relatively well known and will be addressed in the following section. Moreover, changes in subduction parameters have also important consequences in magmatism developed within the overriding plate. Geochemical and isotopic patterns of volcanic rocks can provide ideal opportunities to

constrain cause and effect between tectonics and magmatic activity (e.g., Hildreth and Moorbath, 1988; Gutscher, 2002; Haschke et al., 2006). Therefore, we will compare published geochemical data from arc-related magmatic sequences developed before and during the late Oligocene to early Miocene extensional regime along the Southern Central Andes (27° – 46° S), in order to evaluate the impact of the changing geodynamic setting during these times.

2.1. Late Oligocene to early Miocene extensional intra-arc basins in the Southern Central Andes (27° – 46° S)

The southernmost extensional intra-arc basin among this set

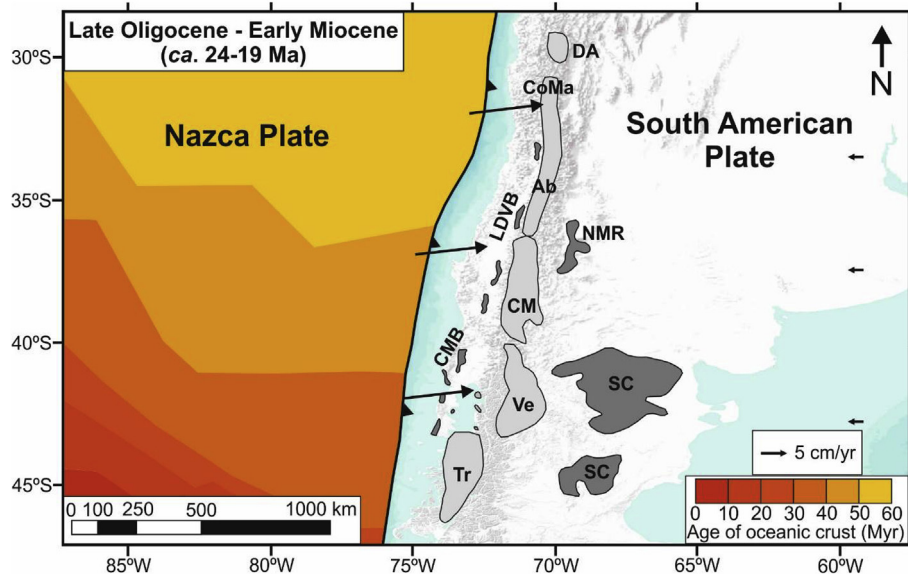


Fig. 2. Location and geodynamic context of the late Oligocene to early Miocene extensional intra-arc basins (light grey) and magmatic belts and plateaux (dark grey) in the Southern Central Andes (27° – 46° S). SC: Somún Cura; Tr: Traiguén Basin; CMB: Coastal Magmatic Belt; LDVB: Longitudinal Depression Volcanic Belt; Ve: Ventana Basin; CM: Cura Mallín Basin; NMR: Neuquén and Mendoza Retroarc volcanism; Ab: Abanico Basin; CoMa: Coya Machalí Basin; DA: Dona Ana Basin. Extent of basins and magmatism based on Lopez-Escobar and Vergara (1997), Muñoz et al. (2000), Kay and Copeland (2006), Kay et al. (2007), Charrier et al. (2007), Rojas Vera et al. (2010), Ramos et al. (2014), Bechis et al. (2014), Winocur et al. (2015), Encinas et al. (2013, 2016). Geodynamic setting based on Somoza and Ghidella (2012) and Müller et al. (2016).

corresponds to the Traiguén basin, located in the western Andean Cordillera between 44° S and 46° S (Fig. 2) (Hervé et al., 1995; Encinas et al., 2016). Recent studies of this basin show that its infill is composed by interbedded pillow basalts, tuffs, breccias, sandstones and shales, which combined with the presence of slumps, turbidites and paleontological evidence, suggest its deposition in a deep marine environment associated with subaqueous volcanism (Encinas et al., 2016). These authors performed U-Pb dating in detrital zircons, which yielded dates between *ca.* 23 and 26 Ma, indicating a late Oligocene – early Miocene maximum depositional age, which is constrained by a *ca.* 20 Ma age of an intrusion in these deposits (Hervé et al., 2001). Syndepositional geometries associated with normal faults are coeval to subaqueous mafic volcanic rocks, whose signature indicates shallow depth of melting from a depleted mantle source developed within a thin crust setting, supporting extension (Encinas et al., 2016). Since this basin remains submerged up to 42° S, the exposures of its infill are limited. Nevertheless, Encinas et al. (2013) described deep marine deposits, whose accumulation occurred during the late Oligocene – early Miocene interval as a consequence of a marine transgression that might have connected the Pacific and Atlantic oceans (Encinas et al., 2014). Encinas et al. (2016) consider that, due to the areal distribution of this transgression, this must have been the result of a major event of regional subsidence, most probably caused by a widespread episode of extension triggered by slab rollback and vigorous asthenospheric wedge circulation.

To the northeast, located in the present Andean arc and retroarc areas, Bechis et al. (2014) described the presence of fossiliferous marine strata that outcrop between 41° S and 43° S, which form part of a volcano-sedimentary infill of several depocenters included within the Ventana basin (Fig. 2). The age of these marine successions was constrained to the latest Oligocene and early Miocene (23–16 Ma) by U-Pb dating (Bechis et al., 2014). The presence of progressive unconformities associated with normal faults allowed these authors to relate these deposits to a regional extensional tectonic stage that took place during the late Oligocene to early

Miocene. Around 41° S, these sedimentary marine rocks are found interbedded with volcanic rocks such as basaltic andesites, basalts and tuffs. The geochemistry of these rocks shows that their emplacement took place in an arc-like environment within a thin crust (Litvak et al., 2014; Fernández Paz et al., 2017b). Furthermore, Orts et al. (2012, 2015) show extensional structures both in seismic records and in outcrops, associated with extensional growth strata in volcanic and sedimentary units deposited within the southern Ventana basin ($41^{\circ}30'$ – 43° S).

Ramos et al. (2014, 2015) showed through gravity data that the Collón Cura depocenter is the continuation of the extensional Ventana basin up to *ca.* 39° S, although no marine transgressions are registered in these deposits (Fig. 2). García Morabito and Ramos (2012) described lateral thickness variations and progressive unconformities in association with normal faults for these Oligocene – early Miocene volcanic sequences. The northernmost reach of this volcaniclastic basin is constituted by the Aluminé depocenter, where Franzese et al. (2011) recognized the presence of major normal faults controlling the deposition of volcanic rocks with ages that locate them in late Oligocene times.

In the same structural trend, between 36° S and 39° S, this extensional period was recorded in a series of depocenters located both in Chile and Argentina, included in the Cura Mallín basin (Fig. 2) (Suárez and Emparán, 1995; Jordan et al., 2001). The infill of this basin consists mostly of pyroclastic deposits with local lava flows, interbedded with fluvial and lacustrine sediments, holding ages between 27 Ma and 17 Ma (Jordan et al., 2001; Burns et al., 2006; Radic, 2010; Shockley et al., 2012). The extensional evidence in this basin is based mainly in the interpretation of seismic records showing wedge-shaped depocenters 1100–1400 meters thick controlled by high-angle normal faults (Folguera et al., 2010; Rojas Vera et al., 2010). Jordan et al. (2001) interpreted that this basin developed during a phase of moderate extension within the plate margin system, triggered by an increased rate of convergence between the Farallon/Nazca and South American plates.

One of the most studied extensional intra-arc basins in the

Southern Central Andes is the Abanico or Coya Machali basin, which extends from 36°S to 30°S along the international boundary between Argentina and Chile (Fig. 2) (Wyss et al., 1994; Godoy et al., 1999; Charrier et al., 1996, 2002, 2007). These basins' infill consists in a voluminous basaltic to rhyolitic volcanic and sedimentary complex composed of volcanic flows, agglomerates, lithic tuffs, and volcaniclastic and lacustrine sediments cut by dykes (Kay et al., 2005; Muñoz et al., 2006). With local stratigraphic thicknesses of 1300 meters, these outcrops occur in two N-S belts, the eastern and western belts. The western belt is composed mainly of volcanic rocks and has an age that ranges between 27.7 Ma and 20.5 Ma, while the eastern belt is richer in sedimentary rocks and has an age that spans between 37 Ma and 16.1 Ma (Charrier et al., 1996, 2002; Kay et al., 2005; Muñoz et al., 2006). Field evidence of extension of these units involves variable lateral thickness of volcano-sedimentary strata, normal faults and synextensional geometries (Charrier et al., 2002; Jara and Charrier, 2014; Jara et al., 2015). Isotopic signatures of these lavas indicate a tholeiitic arc setting with minimal crustal contamination in a relatively thin crust during an extensional regime (Charrier et al., 2002; Kay et al., 2005).

Continuing to the north, the Doña Ana Group basin (30°–29°S) reflects the widening of the magmatic arc, since it corresponds both to an intra-arc and retroarc basin positions (Litvak et al., 2007; Winocur et al., 2015). A recent review of the stratigraphy of this basin, aided by new and more precise geochronological data, shows that its infill is composed by volcanic and pyroclastic products, as well as clastic and volcaniclastic deposits, yielding ages between 26.1 Ma and 18.1 Ma (Jones et al., 2016). Although Ramos et al. (1989) had proposed an extensional regime in the retroarc at these latitudes, Winocur et al. (2015) were the first to use structural arguments based on sets of extensional faults, growth strata and evidences of synextensional sedimentation during late Oligocene to early Miocene times. Supporting this interpretation, coeval calc-alkaline arc-related magmatism has a geochemical signature that reflects the extensional regime that prevailed during these times, controlling the deposition of the volcano-sedimentary sequences within the Doña Ana basin (Litvak et al., 2007; Winocur et al., 2015; Jones et al., 2016).

2.2. Late Oligocene to early Miocene intra-arc basin magmatism along the Southern Central Andes (27°–46°S)

Contrasting geochemical features are observed between magmatic units erupted during the Eocene to early Oligocene and the ones emplaced within the late Oligocene to early Miocene extensional intra-arc basins. Samples from Auca Pan depocenter at 39°S (~29 Ma, Ramos et al., 2014; Iannelli et al., 2017), older lava sections from the Abanico intra-arc basin (~34–28 Ma; Muñoz et al., 2006; Piquer et al., 2017) and northern Pilcaniyeu Magmatic Belt sequences (44 Ma; Iannelli et al., 2017) represent the geochemical signature of the magmas that evolved before the beginning of the late Oligocene-early Miocene extensional regime. In order to characterize the evolution of magmatic products that took place during the extensional regime, younger samples from the Traiguén basin (~26–20 Ma; Encinas et al., 2016), Cura Mallín basin (~26–22 Ma; Jordan et al., 2001; Kay et al., 2006), younger volcanic levels from the Abanico basin (~23–20 Ma; Muñoz et al., 2006; Kay et al., 2005) and northern coeval units form Doña Ana basin (~21–18 Ma; Litvak et al., 2007; Winocur et al., 2015) were plotted (Fig. 3).

Geochemical variations are clearly observed between the two evaluated magmatic stages (Fig. 3). The younger arc-related units from Cura Mallin, Traiguén, Abanico and Doña Ana basins show higher contribution from slab-fluids and a greater degree of partial melting (Fig. 3a, b and c) than older magmatic units from northern Pilcaniyeu Magmatic Belt (44 Ma), Auca Pan (29 Ma) and Abanico

basin (34–28 Ma). Particularly, early Oligocene arc-related magmatism from the Auca Pan depocenter and the Abanico basin shows contributions from calc-alkaline sources, in contrast to the younger upper Oligocene – lower Miocene volcanism from Cura Mallín, Traiguén and Abanico basins, with a tholeiitic signature (Fig. 3d) (Kay et al., 2005, 2006; Muñoz et al., 2006; Litvak et al., 2014; Iannelli et al., 2017). An exception within this younger magmatism corresponds to the Doña Ana volcanic rocks, with a more arc-like chemical signature, which evolved within a mildly extensional intra-arc setting (Litvak et al., 2007; Winocur et al., 2015).

2.3. Late Oligocene to early Miocene magmatic belts and plateaux along the Southern Central Andes (27°–46°S)

Associated with the development of the intra-arc extensional basins described in the previous sections, late Oligocene to early Miocene Andean magmatism showed an important expansion, represented by a series of magmatic belts and plateaux that outcrop along both the present fore-arc and retroarc domains (Fig. 2). Although normal faulting has not been documented in these late Oligocene to early Miocene volcanic deposits, isotopic analysis ($^{87}\text{Sr}/^{86}\text{Sr}$ vs. ϵNd) from these magmatic sequences show minor interaction with crustal components, consistent with their evolution under an extensional regime (Fig. 4).

The Coastal Magmatic Belt igneous rocks outcrop along the Pacific Coast between 37°S and 43.5°S, west of the main cordillera (Fig. 2) (Muñoz et al., 2000). The extrusive rocks of the mid-Tertiary Coastal Magmatic Belt are interbedded with late Oligocene to early Miocene continental and marine sediments, and their age determinations span from 29 Ma to 18.8 Ma. These rocks have a geochemical signature similar to Andean arc magmas and oceanic island basalts, with isotopic composition suggesting upwelling of a variable asthenospheric mantle source, probably affected by seawater alteration (Fig. 4). Combined with assumed changes in the subduction geometry and an increase in convergence rate during these times, Muñoz et al. (2000) propose an extensional stage during late Oligocene to early Miocene times due to a slab rollback of the Nazca plate, which led to an expansion of the magmatic arc and thinning of the crust.

Overlapping with these igneous rocks, a series of volcanic belts are distributed between 33°S and 42.5°S along the Chilean slope of the Andes, known as the Longitudinal Depression Volcanic Belt (Fig. 2) (Lopez-Escobar and Vergara, 1997). Basalts, andesites and dacites form part of the Longitudinal Depression Volcanic Belt, whose isotopic composition falls mostly within the mantle array (Fig. 4). Although previous studies had assigned these rocks between the Eocene and the Miocene, Lopez-Escobar and Vergara (1997) reported K-Ar ages between 26 and 20 Ma for them, constraining this magmatic event between late Oligocene and early Miocene times.

Further east, between 40.5°S and 46°S and at least at ca. 600 km from the trench, lays one of the largest back-arc mafic volcanic fields in the world, known as the Somún Cura magmatic province (Fig. 2) (Kay et al., 2007). With no clear link to a hotspot track or major extension, Kay et al. (2007) group these volcanic rocks into pre-plateau, plateau and post-plateau, each with a distinctive geochemical signature that reflects the interaction of the subducting oceanic slab and the mantle between 33 Ma and 17 Ma (Fig. 4). This magmatism is attributed to a plume-like mantle upwelling with limited crustal contamination, probably related to disturbances during plate reorganization at a time when the South American plate was nearly stationary over the underlying mantle (Fig. 4) (Kay et al., 2007).

To the north, located also in the back-arc and with no clear evidence of synextensional deposition, lavas erupted in the present-

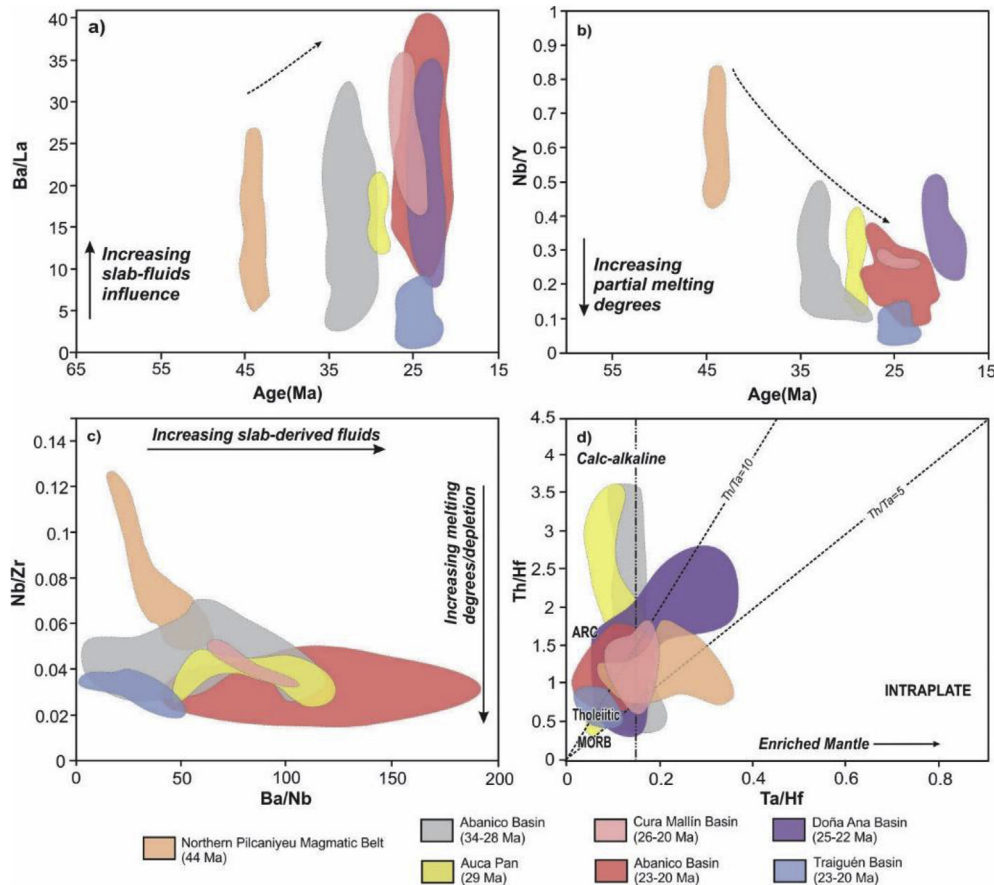


Fig. 3. Comparison of geochemical features between magmatic units erupted before and during the late Oligocene to early Miocene extensional regime. a) Ba/La vs. Age diagram showing the increasing slab-fluid signal after the extensional regime began. b) Decreasing Nb/Y ratios towards younger magmatic units indicate increasing melting degrees after 24–23 Ma. c) Nb/Zr vs. Ba/Nb diagram indicates that younger Abanico volcanic units (23–20 Ma) would present the highest melting degrees and slab-fluid signal. d) Magmas sources would have changed from calc-alkaline to tholeiitic after the onset of the late Oligocene to early Miocene extensional regime. Data sources for the Abanico basin are from Munoz et al. (2006) and Piquer et al. (2017); for the Doña Ana basin are from Litvak et al. (2007) and Winocur et al. (2015); for the Cura Mallin basin are from Kay et al. (2006); for the Traiguén basin are from Encinas et al. (2016); and from Pilcaniyeu Magmatic Belt and Auca Pan are from Iannelli et al. (2017).

day Neuquén and Mendoza retroarc region (35° – 38° S) between 25 Ma and 17 Ma (Fig. 2) (Kay and Copeland, 2006; Silvestro and Atencio, 2009; Dyhr et al., 2013a; 2013b). These successions of volcanic rocks have an isotopic signature with tendency similar to an enriched OIB-like mantle, which became increasingly affected by subduction zone fluids towards the early Miocene (Fig. 4) (Dyhr et al., 2013a; 2013b). Kay and Copeland (2006) interpreted the source of this magmatism in a back-arc mantle devoid of arc-like components, erupted at a time of extension all along the margin due to rollback of the oceanic slab, during a period of rapid, near-normal Nazca-South America plate convergence (Fig. 4).

3. Numerical model and setup

For the numerical modeling experiment we used a 2D improved version of the finite-element code SLIM3D (Popov and Sobolev, 2008; Quinteros and Sobolev, 2012, 2013), which is suitable for simulating the evolution of a subducting slab in a self-consistent manner and has been applied to various extensional and contractional settings (Quinteros et al., 2010; Popov et al., 2012; Brune et al., 2012, 2013, 2014, 2016). The model setup is the same as the Andean subduction reference model from Quinteros and Sobolev (2013), which is characterized by a 2600 km wide and 1200 km deep domain and includes a free surface on the upper side representing topography (model setup and parameters are depicted in

Fig. 5). The overriding plate layers, properties and thicknesses (Fig. 5) are considered suitable for Andean settings between 27° and 46° S, and are explained in detail in the setup of Quinteros and Sobolev (2013) and clarified in the supplementary material.

3.1. Assumptions for the numerical setup

A key input parameter in our model is the beginning of the oceanic slab's subduction, which in our case was set at 30 Ma, simulating the geodynamic setting of South America's western margin (Fig. 1). Based on numerous reconstructions, the Aluk oceanic plate was being subducted beneath South America towards the beginning of the Cenozoic (Fig. 1) (Cande and Leslie, 1986; Somoza and Ghidella, 2005, 2012; Müller et al., 2016). This plate was gradually replaced by the Farallón plate, evidenced by the passage of the Farallón/Aluk mid-ocean ridge (FAMOR) along the Chilean margin at least since ca. 72 Ma (Fig. 1) (Somoza and Ghidella, 2005, 2012; Müller et al., 2016). The southward migration of the FAMOR affected the margin's magmatism and topography (Ramos and Kay, 1992; Arévalo et al., 1994; Ramos, 2005; De la Fuente et al., 2012), ultimately inducing the detachment of the Aluk slab and prompting the opening of a slab window beneath Patagonia at around 56 Ma (Aragón et al., 2011). This scenario, exalted by the prevailing slow and oblique subduction of young and buoyant oceanic lithosphere, would have induced limited

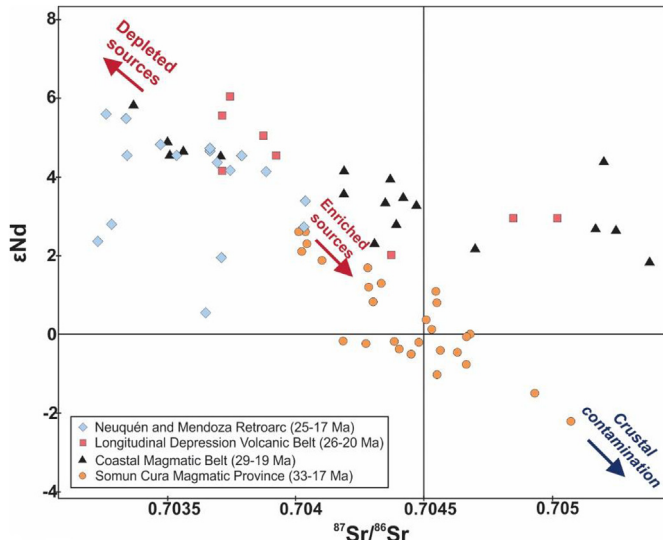


Fig. 4. $^{87}\text{Sr}/^{86}\text{Sr}$ ratios versus ϵNd values for late Oligocene to early Miocene magmatic belts and plateaus present in the Southern Central Andes (27° – 46°S). Compiled data indicate mantelic sources for all samples with minimal crustal contamination. Isotopic data from Neuquén and Mendoza retroarc region correspond to Kay and Copeland (2006) and Dhr et al. (2013a, 2013b); the Longitudinal Depression Volcanic Belt isotopic data are from Lopez-Escobar and Vergara (1997); the Coastal Magmatic Belt isotopic data correspond to Muñoz et al. (2000); the Somún Cura magmatic province data are from Kay et al. (2007).

convergence between the subducting Farallon and overriding South American plates during most of the Paleogene (Fig. 1). Based on the reconstruction of global plate velocities, as well as seismic images, Quinteros and Sobolev (2013) suggested that the tip of the oceanic slab was still in the upper mantle under the central and southern parts of South America by the end of the Eocene. This could be associated with a very oblique and minimized convergence (not enough to form a long slab under South America) and/or the dripping off of the head of the slab into the hot asthenospheric

mantle. The absence of a long slab under the Southern Central Andes resulted in a waning in arc activity and the emplacement of the calc-alkaline Pilcaniyeu Magmatic Belt in the present retroarc area (Rapela et al., 1988; Aragón et al., 2011; Fernández Paz et al., 2017a). Restricted arc-related magmatic products in the Andean arc zone are associated with a slight enriched source and limited slab fluids influence (Fig. 3) (Iannelli et al., 2017). Moreover, limited subsidence in the Southern Central Andes foreland motivated the proposal of a neutral tectonic regime during most of the Paleogene (Horton and Fuentes, 2016). In agreement with this interpretation, seismic studies performed south of the Bolivian orocline demonstrated that alone the Nazca plate seems to be found in the mantle transition zone, although a part of it has already reached the shallower lower mantle (Liu et al., 2003; Pesicek et al., 2012).

Thus, the oceanic slab temperature and thickness correspond to a slab age that ranges between 50 and 40 Myr in accordance with plate reconstructions (Fig. 2), which will decay along the experiment following a standard age cooling model. The simulation involves an initial stage in which the oceanic slab is pushed eastwards at a low velocity (2 cm/yr), in order to approximately mimic the long-lasting oblique or nearly parallel subduction at these latitudes, after the detachment of the Aluk slab. When the slab pull is strong enough to generate a subducting velocity similar to the kinematically imposed velocity, the slab develops dynamically, driven by gravitational instability (Quinteros and Sobolev, 2013). The upper plate is moved westwards throughout the entire simulation, with a change in the imposed velocity from 3 to 2 cm/yr at 10 Ma, in agreement with current reconstructions (Fig. 5) (Somoza and Ghidella, 2012; Colli et al., 2014). Finally, in order for subduction to begin, a low friction subduction channel was incorporated between both plates (Fig. 5) (Sobolev and Babeyko, 2005; Quinteros and Sobolev, 2013).

4. Results

We analyzed the results of Quinteros and Sobolev (2013) model, which has been proven to successfully reproduce the evolution of

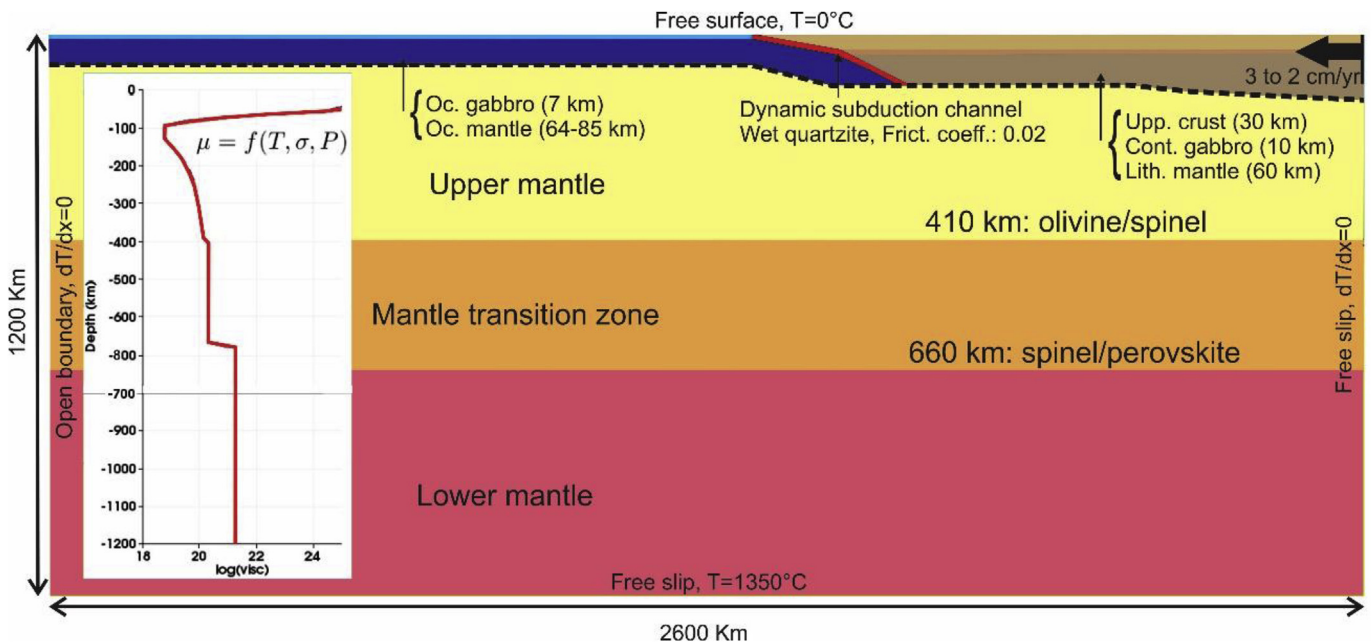


Fig. 5. Model setup and parameters used in the experiment (modified from Quinteros and Sobolev, 2013). Dashed line represents the Lithosphere/Asthenosphere boundary and the inset shows the viscosity profile.

Andean convergence for the last 20 Myr. These authors show that changes in convergence are a natural consequence of the tip of the Nazca plate penetrating into the mantle transition zone and the lower mantle, generating an initial increase followed by a decrease in convergence rate, in coincidence with the growth of the Andes. However, our aim was to start from a setup which includes realistic values for the Oligocene Andean setting, but focusing in the Paleogene–Neogene transition, when the proposed extensional regime occurred. In order to understand the drivers behind this extensional phase and its consequences along the overriding plate, we analyzed Quinteros and Sobolev (2013) model between 24.5 and 17 Ma through changes in topography, isotherms and motion direction.

The model starts at 30 Ma, but since subduction is promoted by the presence of a subduction channel, it requires several Myr in order to equilibrate the initial geometrical setting, lateral strength and density variations. For this reason, the first 5 Myr are not very realistic and aren't taken into account in our analysis. A series of snapshots were taken during the experiment in order to analyze the velocity and temperature variations through time, which are aided by motion direction arrows and location of the 500 °C, 900 °C and 1300 °C isotherms, the last one reflecting the boundary between the lithosphere and the asthenosphere (Fig. 6). A supplementary animation showing the time-evolution of the model can be found at <https://doi.org/10.1016/j.jsames.2017.12.012>.

At the beginning, between 24.5 and 23 Ma, subduction of the oceanic slab is induced simulating ridge push (Fig. 6a), but once the tip of the slab approaches the mantle transition zone at 410 km, it starts to be dynamically driven by gravity due to the influence of the slab pull force (Fig. 6b). Once it enters the mantle transition zone, the increasing downward slab pull produces slab steepening and the retreat of the trench hinge away from the upper plate at around 21.5 Ma (Fig. 6c). The slab continues to be pulled into the mantle transition zone, generating an abrupt increase in convergence velocity at 20 Ma and a vigorous mantle flow into the subduction zone, which affects an 800 km wide zone east of the trench (Fig. 6d). After the oceanic slab reaches the 660 km discontinuity at ca. 18.5 Ma, it has difficulties penetrating into the lower mantle, producing a gradual decrease in the oceanic slab velocity and in the mantle flow towards the asthenospheric wedge (Fig. 6e). In consequence, the slab experiences an upward bending and a decrease in velocity, while a waning in the asthenospheric influx is observed beneath the overriding plate (Fig. 6f).

Although this model is focused mainly in deep mantle processes and does not have a good resolution on topography, it represents a good approximation of what happens to the surface in a regional scale (Fig. 7). In this case, when we analyze the evolution of topography throughout the experiment (surface with $T = 0^\circ\text{C}$) along with isotherm location, we observe that no significant variations occur while the slab is going through the upper mantle between 24.5 and 23 Ma (Fig. 7a and b). However, the initial retreat of the trench hinge and the steepening of the slab observed at 21.5 Ma (Fig. 6c) coincide with the formation of a topographic depression in the overriding plate (Fig. 7c). This process generates localized subsidence, inducing the creation of an intra-arc basin located 200–300 km east of the trench (Fig. 7c and d). Furthermore, the slab steepening creates a void in the mantle wedge beneath the arc, which will be filled by hot asthenospheric material, evidenced by the gradual approach of the isotherms between 23 and 20 Ma (Fig. 7b, c and d). This intra-arc basin, as predicted by the model, reaches its climax and subsides below sea level elevation at ca. 20 Ma, indicating that it can experience marine transgressions, coeval with an asthenospheric influx into the subduction zone (Fig. 7d). Finally, the topography starts to stabilize after 18.5 Ma, and although the depression is

still observable and near sea level, it becomes less pronounced towards the end of the experiment (Fig. 7e and f). This change in topography, along with the gradual decrease in convergence rate, marks the transitional passage between the late Oligocene–early Miocene extensional regime and the Miocene compressional stage that the Andes are still experiencing nowadays, which is analyzed in Quinteros and Sobolev (2013).

5. Discussion

5.1. The role of the slab pull force in the numerical model

Our analysis of Quinteros and Sobolev (2013) experiment shows that the interaction between the Farallon/Nazca oceanic plate and the South American continental plate generated various changes in the geodynamic and tectonic context during late Oligocene and early Miocene times. Among these changes, the most noteworthy are: i) an increase in slab velocity, followed by a gradual decrease; ii) the influx of hot asthenospheric material beneath the overriding plate affecting a 800 km wide zone from the trench towards the craton; iii) the creation of a topographic depression 200–300 km east of the trench.

First, we interpret that the increase in the slab velocity is produced by the slab pull force once the slab interacts with the olivine/spinel transition boundary (410 km). The subsequent velocity decrease reflects the difficulty for the slab to penetrate into the lower mantle as it reaches the spinel/perovskite transition boundary (660 km). Secondly, the asthenospheric influx is generated due to the steepening of the slab, creating a void beneath the overriding plate, inducing the dynamic flow of hot material into the mantle wedge. Once the slab stabilizes its dip angle, a waning in the asthenospheric influx is observed. Finally, the topographic depression is produced by the retreat of the trench hinge away from the overriding plate. This process generates subsidence 200–300 km east of the trench, which is translated as a decrease in elevation and the formation of a basin. The results of the model show that the influence of the slab pull force would be the responsible for the formation of the basin, the increase in convergence velocity and the asthenospheric influx, which would have reached their climax at ca. 20 Ma (Figs. 6d and 7d).

5.2. Comparison of the numerical model with the geological record of the Southern Central Andes (27° – 46°S)

In order to analyze the relationship between the onset of the slab pull force, the sudden increment in velocity, the intra-arc basin formation, crustal stretching and the changes in magma composition in the Southern Central Andes (27° – 46°S), we evaluated a series of properties that could constitute a link between these processes (Fig. 8). The relative length increase in the upper plate was quantified through the stretching factor, which was determined by comparing the length of the deformed continental crust to its initial length. In order to do this, we measured the length of the crust by tracking the position of the trench and the opposite boundary of the continental plate through time. To analyze the topographic response to stretching, we extracted the surface with $T = 0^\circ\text{C}$ from the model and monitored its evolution, which reflected the formation of a basin through time (Fig. 7). To quantify the formation of this basin we calculated its depth, searching for the lowest elevation point of the continental plate and subtracting it to the basin's shoulders elevation. Finally, the velocity of the oceanic plate was extracted directly from the model, and through the addition of the imposed overriding plate's velocity, we obtained the convergence rate (Fig. 8).

When we compare the evolution of these parameters through

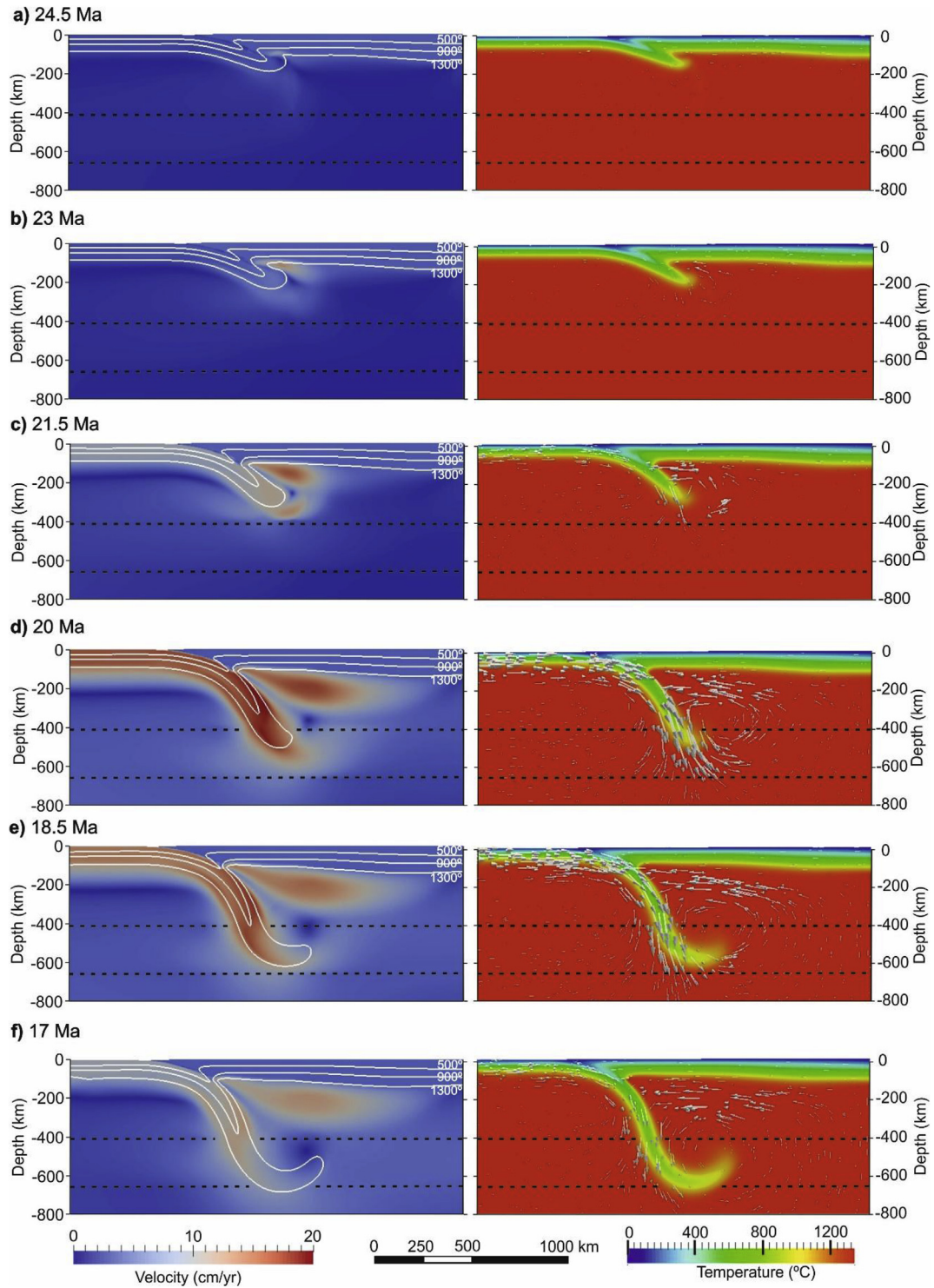


Fig. 6. Evolution of a self-driven Andean reference model based on Quinteros and Sobolev (2013), simulating the subduction of the Farallon/Nazca slab beneath the South American plate between the late Oligocene and the early Miocene. A series of snapshots were taken in order to analyze variations in velocity (left column), temperature and flow direction (right column) during the experiment, focusing in changes occurred once the tip of the oceanic slab enters the mantle transition zone, located between the black dashed lines, representing the 410 km and 660 km phase transitions.

time, we detect a coincidence in their peaks at 20–19 Ma, suggesting a link between them (Fig. 8). After a period of slow subduction, with convergence velocity oscillating between 6 and 8 cm/yr, convergence rate starts to increase as the slab approaches the mantle transition zone at ca. 23 Ma. At the same time, stretching of

the upper crust begins, inducing the formation of a 700 meter deep intra-arc basin as convergence rate reaches its highest value of almost 20 cm/yr at 20 Ma (Fig. 8). This scenario lasts until ca. 19 Ma, when the slab reaches the lower mantle and slows down due to the resistance of the 660 km transition boundary. This event marks the

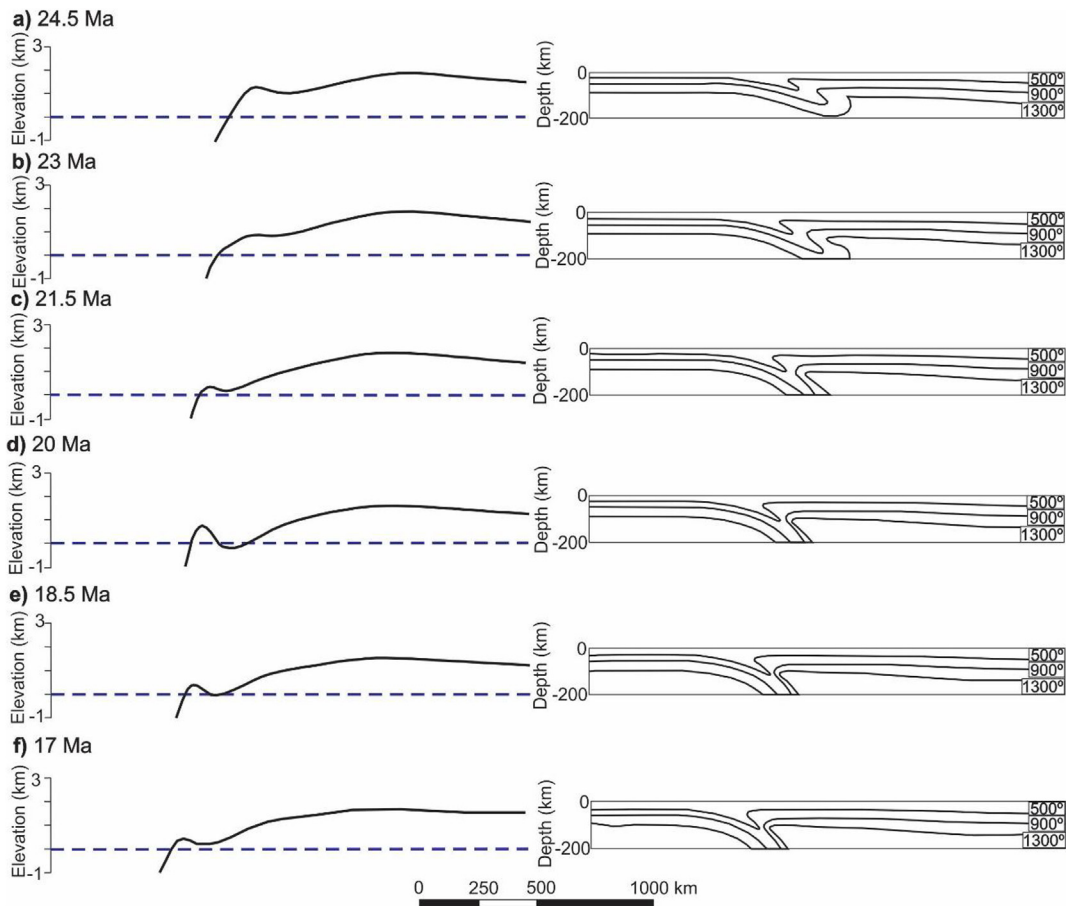


Fig. 7. Evolution of topography (left column, surface with $T = 0^\circ\text{C}$ exaggerated to enhance visibility) and the 500°C , 900°C and 1300°C isotherms location (right column) during the experiment. The formation of a topographic depression and the gradual approach of the isotherms beneath the mantle wedge coincide with the penetration of the slab tip into the mantle transition zone after 23 Ma, as observed in Fig. 6. This induces an asthenospheric influx beneath the overriding plate and the formation of an intra-arc basin located 200–300 km east of the trench, reaching its climax at ca. 20 Ma, when the basin subsides below sea level (depicted by the dashed blue line). (For interpretation of the references to colour in this figure legend, the reader is referred to the Web version of this article.)

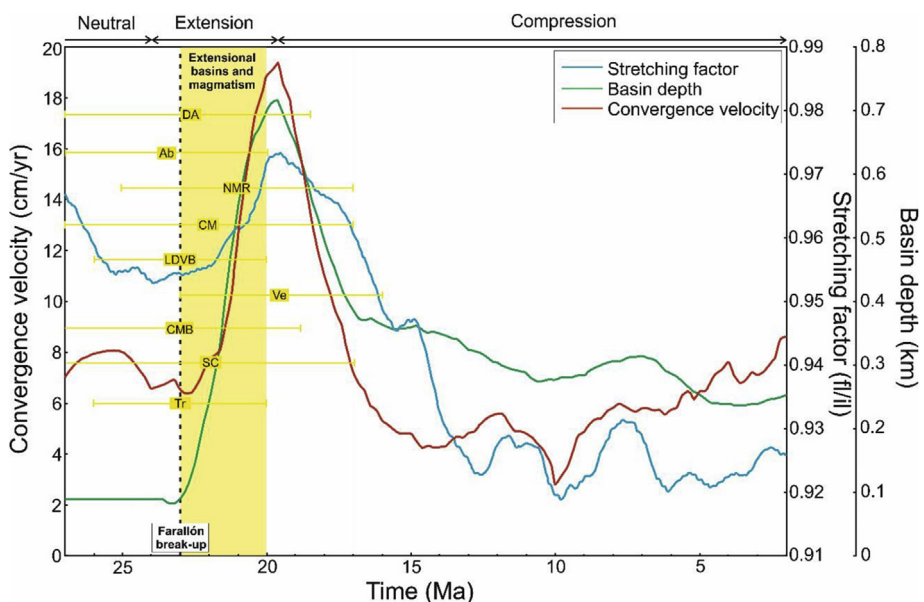


Fig. 8. Evolution of the convergence velocity, stretching of the overriding plate and basin depth through time. Ages of extensional basins and magmatic events between 27° and 46°S are plotted, overlapping between 23 and 20 Ma, which is in agreement with the duration of the extensional regime estimated through our model (references are the same as in Fig. 2). The age of the Farallón break-up (~23 Ma; Lonsdale, 2005) coincides with the increment of velocity and onset of intra-arc basin formation, which suggests a link between the stress exerted by the slab pull force and the partitioning of this plate.

beginning of a gradual decrease in convergence velocity and the onset of shortening in the upper crust, resulting in the shallowing of the basins depth (Fig. 7). The analysis of the changes in convergence rate after this event are discussed and analyzed in Quinteros and Sobolev (2013).

When linking deformation of the upper crust obtained from our model with the tectonic regime, we observe that after a long lived neutral regime in the Southern Central Andes (Horton and Fuentes, 2016), the beginning of an extensional regime occurred at ~24 Ma (Fig. 8). The extensional deformation lasted until 19 Ma, consistent with the formation and development of most of the extensional basins and magmatism recorded between 27° and 46°S along the Andes (Fig. 8). Although their temporal extent varies, when comparing the activity of these basins and duration of the volcanic events, we obtain an overlap between 23 and 20 Ma, in accordance with the results obtained in our model (Fig. 8). Moreover, the beginning of the effect of the slab pull force in our model matches the break-up of the Farallon plate (~23 Ma; Lonsdale, 2005) (Fig. 8), which led Quinteros and Sobolev (2013) to propose that the stress produced by the slab pull force could be the responsible for the splitting of this plate and the birth of the Nazca and Cocos plates. This extensional regime switches towards a compressive regime at approximately 19 Ma, in agreement with the beginning of the present day continuing deformational phase in the Southern Central Andes (Giambiagi et al., 2012; Folguera et al., 2015; Horton and Fuentes, 2016). This last change matches the times of shallowing of the extensional basin observed in our model and the decrease in slab velocity, as depicted by Quinteros and Sobolev (2013).

The behavior of magmatic products during the extensional regime have been proposed to be a consequence of the increase in convergence rate and obliquity, which coincided with the break-up of the Farallon plate at ca. 23 Ma (Iannelli et al., 2017). The late Oligocene to early Miocene episode of trench hinge retreat during the widening of arc-related magmatism between the present fore-arc and retroarc areas cannot be explained by variations in slab dip only, since upwelling of a heat source is required for the widening of the melting zone (Haschke et al., 2006). This heat source would have come from the mix of a previously metasomatized hydrous mantle wedge and a hot asthenospheric influx (Kincaid and Griffiths, 2004), which could explain the higher slab-fluids influence, the greater melting degree and the tholeiitic composition of magmas during the late Oligocene to early Miocene magmatic event. Another explanation for this is the occurrence of a major return flow into the mantle wedge induced by slab rollback, which upgrades the efficiency of decompression melting beneath the fore-arc (Kincaid and Griffiths, 2004). Return flow are known for transporting distinct geochemical and isotopic signatures, which could explain the variable isotopic trends between the distinct intra-arc basins and magmatic belts and plateaux (Pearce et al., 2001). While the variable mantle isotopic signature of the Coastal Magmatic Belt and the Longitudinal Depression Volcanic Belt are explained as the melting of heterogeneous mantle sources (Lopez-Escobar and Vergara, 1997; Muñoz et al., 2000), a transient plume-like mantle upwelling intersecting the subducting plate is proposed for the Somún Cura Magmatic Province in the back-arc area (Fig. 2) (Kay et al., 2007). However, both cases would be a consequence of a mantle instability, such as the one observed in the results of the model (Figs. 6 and 7), which would be associated with the late Oligocene-early Miocene plate reorganization. Changes in volcanism are also observed after ca. 19 Ma, since the volcanic rocks geochemistry shifts towards more andesitic products and a calc-alkaline signature, associated with changes in the slab dip between 28° and 37°S (Kay et al., 2006; Dyrh et al., 2013a and 2013b; Litvak et al., 2017).

5.3. Differences in the impact of the slab pull force along the Southern Central Andes (27°–46°S)

Although a good correlation can be observed between the Southern Central Andes geological record and the area affected by the asthenospheric influx and intra-arc basin formation in our model, the magnitude of extension along basins differs. While calc-alkaline magmatic processes dominate in the northern basins associated with subordinate proximal lacustrine and alluvial sedimentation, marginal and deep sea sedimentation become more important towards the south. The extreme case is represented by the Traiguén and Ventana basins, where deep marine sedimentation and submarine volcanism have been reported by Encinas et al. (2016) and Bechis et al. (2014), respectively.

Since our model is 2-D, only processes taking place along the E-W direction can be considered. Thus, our model would be representing an infinitely wide subduction zone, where no flow of the mantle occurs in N-S direction. Schellart and Moresi (2013), through the analysis of 3-D subduction models, observed the presence of a toroidal mantle flow (parallel to the trench), which favors extensional deformation in narrow slabs and near lateral slab edges. Moreover, these authors observed that the influence of this flow is minimal in the center of wide subduction zones, which serves as a rough approximation of the 2-D models, such as the one presented in this work. This fact, previously analyzed by Schellart (2004) and Piromallo et al. (2006) and observed through parametric studies by Schellart (2008), could be the key to understand the difference in the magnitude of extension throughout the Southern Central Andes between late Oligocene and early Miocene times. Taking this into account, and along with the influence of a previously thickened crust at 30°S (Lossada et al., 2017), we propose that the influence of the extensional regime in the northern basins was less pronounced. On the other hand, the impact of extension was more intense along the southern basins near the slab edge, where it produced the formation of a series of extensional basins beneath sea level, enhanced by the effect of toroidal mantle flow during slab rollback.

6. Conclusions

In this paper we analyze a 2-D self-driven subduction model valid for all Andean settings between 27° and 46°S during late Oligocene and early Miocene times. The results of our model show the onset of an extensional regime at around 24 Ma, which lasted for 5 Myr, in good correlation with the extensional development of intra-arc basins and emplacement of mantle derived volcanic products between these latitudes. Climax of extensional deformation at ca. 20 Ma coincides with a hot asthenospheric influx affecting an 800 km wide zone east of the trench and the opening of a 700 m deep intra-arc basin located 200–300 km east of the limit between the oceanic and continental plates. These processes are associated with the influence of the slab pull force, generated by the approach of the oceanic slab towards the mantle transition zone at ca. 23 Ma. After a period of slow and oblique subduction that lasted for most of the Paleogene, the influence exerted by the slab pull force generated an abrupt increment in convergence rate and a more orthogonal subduction along South America's western margin. The initial influence of the slab pull force resulted in the steepening of the slab and the retreat of the trench hinge away from the upper plate towards the beginning of the Neogene. This caused the formation of an intra-arc basin and an influx of hot material beneath the continental plate. Around 19 Ma, the tip of the slab encounters resistance as it enters the lower mantle, which translates into a gradual decrease in convergence rate, a waning in the asthenospheric influx and the passage towards a compressional

regime, resulting in a more calc-alkaline geochemistry in volcanic products and the initiation of a new contractional phase in the Andes as registered synorogenic sedimentation indicates.

The activity of extensional basins and the duration of magmatic events in the Southern Central Andes (27° – 46° S) overlap roughly between 23 and 20 Ma, in good accordance with our results. Although the area of effect of the asthenospheric influx would explain mantle derived magmatism in the present Andean retroarc up to 800 km east of the trench, the impact of this extensional regime along the intra-arc basins between 27° and 46° S was not homogeneous. Differences in crustal thickness prior to the extensional regime and the effect of toroidal mantle flow near the southern slab edge could be the responsible for the variations in the impact of the slab pull force along the Southern Central Andes.

Acknowledgements

We acknowledge Marius Walter and the GFZ Geodynamic modeling section for their support during the corresponding author's three month stay as part of a collaboration project between CONICET and Helmholtz Association entitled "Geodynamic evolution of the Neuquén Andes: implications for Geo-Resources". We would like to particularly acknowledge Nick Perez, Sascha Brune and Muriel Gerbault for their helpful revisions, which served to greatly improve an early version of this manuscript. This work has been possible through the financial support of the Helmholtz Association (grant HIRG-0008) and CONICET (grant PIP 2015–2017 11220150100426). This is the contribution R-242 of the Instituto de Estudios Andinos "Don Pablo Groeber".

Appendix A. Supplementary data

Supplementary data related to this article can be found at <https://doi.org/10.1016/j.jsames.2017.12.012>.

References

- Allmendinger, R.W., Jordan, T.E., Kay, S.M., Isacks, B.L., 1997. The evolution of the altiplano-puna plateau of the central Andes. *Annu. Rev. Earth Planet Sci.* 25 (1), 139–174.
- Agarón, E., D'Eramo, F., Castro, A., Pinotti, L., Brunelli, D., Rabbia, O., Rivalenti, G., Varela, R., Spakman, W., Demartis, M., Cavarozzi, C.E., Aguilera, Y.E., Mazzucchelli, M., Ribot, A., 2011. Tectono-magmatic response to major convergence changes in the North Patagonian suprasubduction system; the Paleogene subduction-transcurrent plate margin transition. *Tectonophysics* 509, 218–237.
- Arévalo, C., Rivera, O., Iriarte, S., Mpodozis, C., 1994. Cuencas extensionales y campos de calderas del Cretácico superior-Terciario inferior en la precordillera de Copiapo (27° – 28° S), Chile. In: Actas VIIº Congreso Geológico Chileno, 2, pp. 1288–1292.
- Baby, P., Hérai, G., Salinas, R., Sempere, T., 1992. Geometry and kinematic evolution of passive roof duplexes deduced from cross section balancing: example from the foreland thrust system of the southern Bolivian Subandean Zone. *Tectonics* 11 (3), 523–536.
- Bechis, F., Encinas, A., Concheyro, A., Litvak, V.D., Aguirre-Urreta, B., Ramos, V.A., 2014. New age constraints for the Cenozoic marine transgressions of northwestern Patagonia, Argentina (41° – 43° S): paleogeographic and tectonic implications. *J. S. Am. Earth Sci.* 52, 72–93.
- Blisniuk, P.M., Stern, L.A., Chamberlain, C.P., Idleman, B., Zeitler, P.K., 2005. Climatic and ecologic changes during Miocene surface uplift in the southern patagonian Andes. *Earth Planet Sci. Lett.* 230 (1), 125–142.
- Brune, S., Popov, A.A., Sobolev, S.V., 2012. Modeling suggests that oblique extension facilitates rifting and continental break-up. *J. Geophys. Res.: Solid Earth* 117, B08402. <https://doi.org/10.1029/2011JB008860>.
- Brune, S., Popov, A.A., Sobolev, S.V., 2013. Quantifying the thermo-mechanical impact of plume arrival on continental break-up. *Tectonophysics* 604, 51–59.
- Brune, S., Heine, C., Pérez-Gussinyé, M., Sobolev, S.V., 2014. Rift migration explains continental margin asymmetry and crustal hyper-extension. *Nat. Commun.* 5.
- Brune, S., Williams, S.E., Butterworth, N.P., Müller, R.D., 2016. Abrupt plate accelerations shape rifted continental margins. *Nature* 536 (7615), 201–204.
- Burns, W.M., Jordan, T.E., Copeland, P., Kelley, S.A., 2006. The case for extensional tectonics in the Oligocene-Miocene Southern Andes as recorded in the Cura Mallín basin (36° – 38° S). In: Kay, S.M., Ramos, V.A. (Eds.), *Evolution of an Andean Margin: a Tectonic and Magmatic View from the Andes to the Neuquén Basin (35° – 39° S Lat)*, vol. 407. Geological Society of America Special Papers, pp. 163–184.
- Cande, S.C., Leslie, R.B., 1986. Late Cenozoic tectonics of the southern Chile trench. *J. Geophys. Res.: Solid Earth* 91 (B1), 471–496.
- Capitanio, F.A., Faccenna, C., Zlotnik, S., Stegman, D.R., 2011. Subduction dynamics and the origin of Andean orogeny and the Bolivian orocline. *Nature* 480 (7375), 83–86.
- Charrier, R., Wyss, A.R., Flynn, J.J., Swisher, C.C., Norell, M.A., Zapatta, F., McKenna, M.C., Novacek, M.J., 1996. New evidence for late mesozoic-early cenozoic evolution of the chilean Andes in the upper tinguiricá valley (35° S), Central Chile. *J. S. Am. Earth Sci.* 9 (5), 393–422.
- Charrier, R., Baeza, O., Elgueta, S., Flynn, J.J., Gans, P., Kay, S.M., Muñoz, N., Wyss, A.R., Zurita, E., 2002. Evidence for Cenozoic extensional basin development and tectonic inversion south of the flat-slab segment, southern Central Andes, Chile (33° – 36° SL). *J. S. Am. Earth Sci.* 15 (1), 117–139.
- Charrier, R., Pinto, L., Rodríguez, M.P., 2007. Tectonostratigraphic evolution of the andean orogen in Chile. In: Moreno, T., Gibbons, W. (Eds.), *The Geology of Chile*. The Geological Society of London, London, UK, pp. 21–114.
- Charrier, R., Ramos, V.A., Tapia, F., Sagripanti, L., 2015. Tectono-stratigraphic evolution of the andean orogen between 31° and 37° S (Chile and western Argentina). In: Sepúlveda, S.A., Giambiagi, L.B., Moreiras, S.M., Pinto, L., Tunik, M., Hoke, G.D., Farías, M. (Eds.), *Geodynamic Processes in the Andes of Central Chile and Argentina*, vol. 399. The Geological Society of London, London, UK, pp. 13–61. Special Publications.
- Corpa, N.G., Hassani, R., Gerbault, M., Prévost, J.H., 2014. A fictitious domain method for lithosphere-asthenosphere interaction: application to periodic slab folding in the upper mantle. *G-cubed* 15 (5), 1852–1877.
- Corpa, N.G., Araya, R., Gerbault, M., Hassani, R., 2015. Relationship between slab dip and topography segmentation in an oblique subduction zone: insights from numerical modeling. *Geophys. Res. Lett.* 42 (14), 5786–5795.
- Cobbold, P.R., Rosello, E.A., 2003. Aptian to recent compressional deformation, foothills of the Neuquén Basin, Argentina. *Mar. Petrol. Geol.* 20, 429–443.
- Colli, L., Stotz, I., Bunge, H.P., Smethurst, M., Clark, S., Iaffaldano, G., Tassara, A., Guillocheau, F., Bianchi, M.C., 2014. Rapid South Atlantic spreading changes and coeval vertical motion in surrounding continents: evidence for temporal changes of pressure-driven upper mantle flow. *Tectonics* 33 (7), 1304–1321.
- Coney, P.J., Evenchick, C.A., 1994. Consolidation of the american cordilleras. *J. S. Am. Earth Sci.* 7 (3–4), 241–262.
- DeCelles, P.G., Ducea, M.N., Kapp, P., Zandt, G., 2009. Cyclicity in Cordilleran orogenic systems. *Nat. Geosci.* 2 (4), 251–257.
- De la Fuente, D., Figueroa, O., Duhart, P., Quiroz, D., Demaiffe, D., Oliveros, V., Muñoz, J., 2012. Los intrusivos de Antearco del Cretácico Superior de Chile Centro Sur (39° S– 40° S): petrografía y geoquímica. In: *Actas XIII Congreso Geológico Chileno*, pp. 342–344.
- Dyhr, C.T., Holm, P.M., Llambías, E.J., Scherstén, A., 2013a. Subduction controls on Miocene back-arc lavas from Sierra de Huantacocha and La Matancilla and new 40 Ar/ 39 Ar dating from the Mendoza Region, Argentina. *Lithos* 179, 67–83.
- Dyhr, C.T., Holm, P.M., Llambías, E.J., 2013b. Geochemical constraints on the relationship between the Miocene–Pliocene volcanism and tectonics in the Palaoco and Fortunoso volcanic fields, Mendoza Region, Argentina: new insights from 40 Ar/ 39 Ar dating, Sr–Nd–Pb isotopes and trace elements. *J. Volcanol. Geoth. Res.* 266, 50–68.
- Echaurren, A., Folguera, A., Gianni, G., Orts, D., Tassara, A., Encinas, A., Tassara, A., Giménez, M., Valencia, V., 2016. Tectonic evolution of the North Patagonia Andes (41° – 44° S) through recognition of syntectonic strata. *Tectonophysics* 677–678, 99–114.
- Encinas, A., Zambrano, P.A., Finger, K.L., Valencia, V., Buatois, L.A., Duhart, P., 2013. Implications of deep-marine Miocene deposits on the evolution of the north patagonian Andes. *J. Geol.* 121, 215–238.
- Encinas, A., Pérez, F., Nielsen, S.N., Finger, K.L., Valencia, V., Duhart, P., 2014. Geochronologic and paleontologic evidence for a pacific-atlantic connection during the late oligocene–early Miocene in the patagonian Andes (43 – 44° S). *J. S. Am. Earth Sci.* 55, 1–18.
- Encinas, A., Folguera, A., Oliveros, V., Del Mauro, L.D.G., Tapia, F., Riff, R., Hervé, F., Finger, K.L., Valencia, V.A., Gianni, G., Alvarez, O., 2016. Late Oligocene–early Miocene submarine volcanism and deep-marine sedimentation in an extensional basin of southern Chile: implications for the tectonic development of the North Patagonian Andes. *Geol. Soc. Am. Bull.* 128 (5–6), 807–823. <https://doi.org/10.1130/B313031>.
- Esprut, N., Funiciello, F., Martinod, J., Guillaume, B., Regard, V., Faccenna, C., Brunet, S., 2008. Flat subduction dynamics and deformation of the South American plate: insights from analog modeling. *Tectonics* 27, 3.
- Fernández Paz, L., Litvak, V.D., Echaurren, A., Iannelli, S.B., Encinas, A., Folguera, A., Valencia, V., 2017. Late Eocene volcanism in north Patagonia (42° – 30° – 43° S): arc resumption after a stage of within-plate magmatism. *J. Geodyn.* 113, 13–31.
- Fernández Paz, L., Bechis, F., Litvak, V.D., Echaurren, A., Iannelli, S., Encinas, A., Oliveros, V., Folguera, A., Valencia, V., 2017b. Evolución del volcanismo de arco durante el Eocene medio-Mioceno temprano en los Andes Patagónicos. In: *Actas XX Congreso Geológico Argentino*, p. 6.
- Folguera, A., Ramos, V.A., 2011. Repeated eastward shifts of arc magmatism in the Southern Andes: a revision to the long-term pattern of Andean uplift and magmatism. *J. S. Am. Earth Sci.* 32 (4), 531–546.
- Folguera, A., Rojas Vera, E.A., Bottesi, G., Zamora Valcarce, G., Ramos, V.A., 2010. The Loncopué trough: a cenozoic basin produced by extension in the southern

- central Andes. *J. Geodyn.* 49 (5), 287–295.
- Folguera, A., Naipauer, M., Sagripanti, L., Chiglione, M., Orts, D.L., Giambiagi, L., 2015. Growth of the Southern Andes. Springer Earth System Sciences. <https://doi.org/10.1007/978-3-319-23060-3>.
- Franzese, J.R., D'Elia, L., Bilmes, A., Muravchik, M., Hernández, M., 2011. Superposición de cuencas extensionales y contraccionales oligo-miocenas en el retroarco andino norpatagónico: la Cuenca de Aluminé, Neuquén, Argentina. *Andean Geol.* 38 (2), 319–334.
- Gansser, A., 1973. Facts and theories on the Andes. *J. Geol. Soc.* 129, 170–191.
- García Morabito, E., Ramos, V.A., 2012. Andean evolution of the Aluminé fold and thrust belt, northern patagonian Andes (38°30'–40°30'S). *J. S. Am. Earth Sci.* 38, 13–30.
- Garzione, C.N., Hoke, G.D., Libarkin, J.C., Withers, S., MacFadden, B., Eiler, J., Ghosh, P., Mulch, A., 2008. Rise of the Andes. *Science* 320 (5881), 1304–1307.
- Gerbault, M., Cembrano, J., Mpodozis, C., Farias, M., Pardo, M., 2009. Continental margin deformation along the Andean subduction zone: thermo-mechanical models. *Phys. Earth Planet. In.* 177 (3), 180–205.
- Giambiagi, L., Mescua, J., Bechis, F., Tassara, A., Hoke, G., 2012. Thrust belts of the southern Central Andes: along-strike variations in shortening, topography, crustal geometry, and denudation. *Geol. Soc. Am. Bull.* 124 (7–8), 1339–1351.
- Gibert, G., Gerbault, M., Hassani, R., Tric, E., 2012. Dependency of slab geometry on absolute velocities and conditions for cyclicity: insights from numerical modelling. *Geophys. J. Int.* 189 (2), 747–760.
- Giovanni, M.K., Horton, B.K., Garzione, C.N., McNulty, B., Grove, M., 2010. Extensional basin evolution in the Cordillera Blanca, Peru: stratigraphic and isotopic records of detachment faulting and orogenic collapse in the Andean hinterland. *Tectonics* 29 (6), TC6007. <https://doi.org/10.1029/2010TC002666>.
- Gillis, R.J., Horton, B.K., Grove, M., 2006. Thermochronology, geochronology, and upper crustal structure of the Cordillera Real: implications for Cenozoic exhumation of the central Andean plateau. *Tectonics* 25, TC6007. <https://doi.org/10.1029/2005TC001887>.
- Godoy, E., Yáñez, G., Vera, E., 1999. Inversion of an Oligocene volcano-tectonic basin and uplifting of its superimposed Miocene magmatic arc in the Chilean Central Andes: first seismic and gravity evidences. *Tectonophysics* 306 (2), 217–236.
- Gripp, A.E., Gordon, R.G., 2002. Young tracks of hotspots and current plate velocities. *Geophys. J. Int.* 150, 321–361. <https://doi.org/10.1046/j.1365-264X.2002.01627.x>.
- Gutscher, M.A., 2002. Andean subduction styles and their effect on thermal structure and interplate coupling. *J. S. Am. Earth Sci.* 15 (1), 3–10.
- Haschke, M., Günther, A., Melnick, D., Echtler, H., Reutter, K.J., Scheuber, E., Oncken, O., 2006. Central and southern Andean tectonic evolution inferred from arc magmatism. In: Oncken, O., Chong, G., Franz, G., Giese, P., Gotze, H.J., Ramos, V.A., Strecker, M.R., Wigger, P. (Eds.), *The Andes*, vol. 22. Springer, Berlin, Heidelberg, pp. 337–353.
- Hervé, F., Pankhurst, R.J., Drake, R., Beck, M.E., 1995. Pillow metabasalts in a mid-tertiary extensional basin adjacent to the Liquiñe-Ofoqui fault zone: the Isla Magdalena area, Aysén, Chile. *J. S. Am. Earth Sci.* 8 (1), 33–46.
- Hervé, F., Sanhueza, A., Silva, C., Pankhurst, R.J., Fanning, M.C., Campbell, H., Crundwell, M., 2001. A Neogene age for Traiguén Formation, Aysén, Chile, as revealed by SHRIMP U-Pb dating of detrital zircons. In: *Actas III Simposio Sudamericano de Geología Isotópica*. Pucón, Chile. Servicio Nacional de Geología y Minería, pp. 570–574.
- Heuret, A., Lallemand, S., 2005. Plate motions, slab dynamics and back-arc deformation. *Phys. Earth Planet. In.* 149 (1), 31–51.
- Hildreth, W., Moorbath, S., 1988. Crustal contributions to arc magmatism in the Andes of central Chile. *Contrib. Mineral. Petrol.* 98 (4), 455–489.
- Hoke, G.D., Giambiagi, L.B., Garzione, C.N., Mahoney, J.B., Strecker, M.R., 2014. Neogene paleoelevation of intermontane basins in a narrow, compressional mountain range, southern Central Andes of Argentina. *Earth Planet. Sci. Lett.* 406, 153–164.
- Horton, B.K., 2005. Revised deformation history of the central Andes: inferences from Cenozoic foredeep and intermontane basins of the Eastern Cordillera, Bolivia. *Tectonics* 24, TC3011. <https://doi.org/10.1029/2003TC001619>.
- Horton, B.K., Fuentes, F., 2016. Sedimentary record of plate coupling and decoupling during growth of the Andes. *Geology* 44 (8), 647–650.
- Horton, B.K., Fuentes, F., Boll, A., Starck, D., Ramirez, S.G., Stockli, D.F., 2016. Andean stratigraphic record of the transition from backarc extension to orogenic shortening: a case study from the northern Neuquén Basin, Argentina. *J. S. Am. Earth Sci.* 71, 17–40.
- Iannelli, S.B., Litvak, V.D., Fernández Paz, L., Folguera, A., Ramos, M.E., Ramos, V.A., 2017. Evolution of Eocene to Oligocene arc-related volcanism in the north patagonian Andes (39°–41°S), prior to the break-up of the Farallón plate. *Tectonophysics* 696–697, 70–87.
- James, D.E., Sacks, I.S., 1999. Cenozoic formation of the Central Andes: a geophysical perspective. *Geol. ore deposits of the Central Andes* 7, 1–25.
- Jara, P., Charrier, R., 2014. Nuevos antecedentes estratigráficos y geocronológicos para el Meso-Cenozoico de la Cordillera Principal de Chile entre 32° y 32° 30'S: implicancias estructurales y paleogeográficas. *Andean Geol.* 41 (1), 174–209.
- Jara, P., Likerman, J., Winocur, D., Ghiglione, M.C., Cristallini, E.O., Pinto, L., Charrier, R., 2015. Role of basin width variation in tectonic inversion: insight from analogue modelling and implications for the tectonic inversion of the Abanico Basin, 32°–34° S, Central Andes. In: Sepúlveda, S.A., Giambiagi, L.B., Moreiras, S.M., Pinto, L., Tunik, M., Hoke, G.D., Farias, M. (Eds.), *Geodynamic Processes in the Andes of Central Chile and Argentina*, vol. 399. The Geological Society of London, London, UK, pp. 83–107. Special Publications.
- Jones, R.E., Kirstein, L.A., Kasemann, S.A., Litvak, V.D., Poma, S., Elliott, T., Alonso, R., Hinton, R., EIMF, 2016. The role of changing geodynamics in the progressive contamination of Late Cretaceous to Late Miocene arc magmas in the southern Central Andes. *Lithos* 169–191.
- Jordan, T.E., Burns, W.M., Veiga, R., Pángaro, F., Copeland, P., Kelley, S., Mpodozis, C., 2001. Extension and basin formation in the southern Andes caused by increased convergence rate: a mid-Cenozoic trigger for the Andes. *Tectonics* 20 (3), 308–324.
- Kay, S.M., Copeland, P., 2006. Early to middle Miocene backarc magmas of the Neuquén Basin: geochemical consequences of slab shallowing and the westward drift of South America. *Geol. Soc. Am. Special Pap.* 407, 185–213.
- Kay, S.M., Godoy, E., Kurtz, A., 2005. Episodic arc migration, crustal thickening, subduction erosion, and magmatism in the south-central Andes. *Geol. Soc. Am. Bull.* 117 (1–2), 67–88.
- Kay, S.M., Burns, M., Copeland, P., 2006. Upper Cretaceous to Holocene magmatism and evidence for transient Miocene shallowing of the Andean subduction zone under the northern Neuquén Basin. In: Kay, S.M., Ramos, V.A. (Eds.), *Evolution of an Andean Margin: a Tectonic and Magmatic View from the Andes to the Neuquén Basin (35°–39°S)*, vol. 407. Geological Society of America, USA, pp. 19–60. Special Papers.
- Kay, S.M., Ardolino, A.A., Gorring, M.L., Ramos, V.A., 2007. The Somuncura Large Igneous Province in Patagonia: interaction of a transient mantle thermal anomaly with a subducting slab. *J. Petrol.* 48 (1), 43–77.
- Kincaid, C., Griffiths, R.W., 2004. Variability in flow and temperatures within mantle subduction zones. *G-cubed* 5 (6), Q06002. <https://doi.org/10.1029/2003GC000666>.
- Kley, J., Monaldi, C.R., Salinity, J.A., 1999. Along-strike segmentation of the Andean foreland: causes and consequences. *Tectonophysics* 301 (1), 75–94.
- Litvak, V.D., Poma, S., Kay, S.M., 2007. Paleogene and Neogene magmatism in the Valle del Cura region: new perspective on the evolution of the Pampean flat slab, San Juan province, Argentina. *J. S. Am. Earth Sci.* 24, 117–137.
- Litvak, V.D., Encinas, A., Oliveros, V., Bechis, F., Folguera, A., y Ramos, V.A., 2014. El volcanismo mioceno inferior vinculado con las ingestiones marinas en los Andes Nordpatagónicos. In: *Actas XIX Congreso Geológico Argentino*, pp. S22–S35.
- Litvak, V.D., Spagnuolo, M.G., Folguera, A., Poma, S., Jones, R., Ramos, V.A., 2015. Late Cenozoic calc-alkaline volcanism over the Payenia shallow subduction zone, South-Central Andean back-arc (34°30'–37°S), Argentina. *J. S. Am. Earth Sci.* 64 (2), 365–380.
- Litvak, V.D., Poma, S., Jones, R.E., Fernández Paz, L., Iannelli, S.B., Spagnuolo, M., Kirstein, L.A., Folguera, A., Ramos, V.A., 2017. The late Paleogene to Neogene volcanic arc in the southern central Andes (28°–37°S). In: Folguera, A., Contreras Reyes, E., Heredia, N., Encinas, A., Iannelli, S., Oliveros, V., Dávila, F., Collo, G., Giambiagi, L., MakSYMowicz, A., Iglesia Llanos, P., Turienzo, M., Naipauer, M., Orts, D., Litvak, V., Alvarez, O., Arriagada, C. (Eds.), *The Evolution of the Chilean-Argentinean Andes*. Springer Earth System Sciences.
- Liu, K.H., Gao, S.S., Silver, P.G., Zhang, Y., 2003. Mantle layering across central South America. *J. Geophys. Res.* 108, 2510. <https://doi.org/10.1029/2002JB002208>.
- Lonsdale, P., 2005. Creation of the Cocos and Nazca plates by fission of the Farallon plate. *Tectonophysics* 404, 237–264. <https://doi.org/10.1016/j.tecto.2005.05.011>.
- López-Escobar, L., Vergara, M., 1997. Eocene–Miocene longitudinal depression and Quaternary volcanism in the Southern Andes, Chile (33°–42.5°S): a geochemical comparison. *Rev. Geol. Chile* 24 (2), 227–244.
- Lossada, A.C., Giambiagi, L., Hoke, G.D., Fitzgerald, P.G., Creixell, C., Murillo, I., Mardonez, D., Velásquez, R., Suriano, J., 2017. Thermochronologic evidence for late Eocene Andean mountain building at 30°S. *Tectonics* 36 (11), 2693–2713.
- Maloney, K.T., Clarke, G.L., Klepeis, K.A., Quevedo, L., 2013. The Late Jurassic to present evolution of the Andean margin: drivers and the geological record. *Tectonics* 32. <https://doi.org/10.1002/tect.20067>.
- Manea, V.C., Pérez-Gussinyé, M., Manea, M., 2012. Chilean flat slab subduction controlled by overriding plate thickness and trench rollback. *Geology* 40 (1), 35–38.
- Manea, V.C., Manea, M., Ferrari, L., Orozco, T., Valenzuela, R.W., Husker, A., Kostoglodov, V., 2017. A review of the geodynamic evolution of flat slab subduction in Mexico, Peru, and Chile. *Tectonophysics* 695, 27–52.
- Marrett, R., Strecker, M.R., 2000. Response of intracontinental deformation in the central Andes to late Cenozoic reorganization of South American Plate motions. *Tectonics* 19 (3), 452–467.
- McNulty, B., Farber, D., 2002. Active detachment faulting above the Peruvian flat slab. *Geology* 30 (6), 567–570.
- McQuarrie, N., Horton, B.K., Zandt, G., Beck, S., DeCelles, P.G., 2005. Lithospheric evolution of the Andean fold-thrust belt, Bolivia, and the origin of the Central Andean plateau. *Tectonophysics* 399, 15–37.
- McQuarrie, N., Barnes, J.B., Ehlers, T.A., 2008. Geometric, kinematic, and erosional history of the central Andean Plateau, Bolivia (15°–17°S). *Tectonics* 27, 3.
- Mora, A., Parra, M., Strecker, M.R., Kammer, A., Dimaté, C., Rodríguez, F., 2006. Cenozoic contractional reactivation of Mesozoic extensional structures in the Eastern Cordillera of Colombia. *Tectonics* 25, 2.
- Mpodozis, C., Allmendinger, R.W., 1993. Extensional tectonics, cretaceous Andes, northern Chile (27°S). *Geol. Soc. Am. Bull.* 105 (11), 1462–1477.
- Müller, R.D., Seton, M., Zahirovic, S., Williams, S.E., Matthews, K.J., Wright, N.M.,

- Shephard, G.E., Maloney, K.T., Barnett-Moore, N., Hosseinpour, M., Bower, D.J., Cannon, J., 2016. Ocean basin evolution and global-scale plate reorganization events since Pangea breakup. *Annu. Rev. Earth Planet Sci.* 44 (1), 107–138.
- Muñoz, J., Troncoso, R., Duhart, P., Crignola, P., Farmer, L., Stern, C.R., 2000. The relation of the mid-Tertiary coastal magmatic belt in south-central Chile to the late Oligocene increase in plate convergence rate. *Rev. Geol. Chile* 27 (2), 177–203.
- Muñoz, M., Fuentes, F., Vergara, M., Aguirre, L., Olov Nyström, J., Féraud, G., Demant, A., 2006. Abanico East Formation: petrology and geochemistry of volcanic rocks behind the Cenozoic arc front in the Andean Cordillera, central Chile (33°–50°S). *Rev. Geol. Chile* 331, 109–140.
- Noury, M., Philippon, M., Bernet, M., Paquette, J.L., Sempere, T., 2017. Geological record of flat slab–induced extension in the southern Peruvian forearc. *Geology* G38990–G38991.
- O'Driscoll, L.J., Richards, M.A., Humphreys, D.E., 2012. Nazca–South America interactions and the late Eocene–late Oligocene flat-slab episode in the central Andes. *Tectonics* 31, TC2013. <https://doi.org/10.1029/2011TC003036>.
- Oncken, O., Hindle, D., Kley, J., Elger, K., Victor, P., Schemann, K., 2006. Deformation of the Central Andean upper plate system – facts, fiction, and constraints for plateau models. In: Oncken, O., Chong, G., Franz, G., Giese, P., Gotze, H.J., Ramos, V.A., Strecker, M.R., Wigger, P. (Eds.), *The Andes*, vol. 22. Springer, Berlin, Heidelberg, pp. 3–27.
- Orts, D.L., Folguera, A., Encinas, A., Ramos, M., Tobal, J., Ramos, V.A., 2012. Tectonic development of the North Patagonian Andes and their related Miocene foreland basin (41°–30°–43° S). *Tectonics* 31, TC3012. <https://doi.org/10.1029/2011TC003084>.
- Orts, D.L., Folguera, A., Giménez, M., Ruiz, F., Rojas Vera, E.A., Klinger, F.L., 2015. Cenozoic building and deformational processes in the north patagonian Andes. *J. Geodyn.* 86, 26–41.
- Pardo-Casas, F., Molnar, P., 1987. Relative motion of the Nazca (Farallon) and south american plates since late cretaceous time. *Tectonics* 6 (3), 233–248.
- Pearce, J.A., Leat, P.T., Barker, P.F., Millar, I.L., 2001. Geochemical tracing of pacific-to-atlantic upper-mantle flow through the drake passage. *Nature* 410 (6827), 457–461.
- Pesicek, J.D., Engdahl, E.R., Thurber, C.H., DeShon, H.R., Lange, D., 2012. Mantle subducting slab structure in the region of the 2010 M8.8 Maule earthquake (30°–40°S), Chile. *Geophys. J. Int.* 191, 317–324. <https://doi.org/10.1111/j.1365-246X.2012.05624.x>.
- Piquer, J., Hollings, P., Rivera, O., Cooke, D.R., Baker, M., Testa, F., 2017. Along-strike segmentation of the Abanico basin, central Chile: new chronological, geochemical and structural constraints. *Lithos* 268–271, 174–197.
- Piromallo, C., Becker, T.W., Funiciello, F., Faccenna, C., 2006. Three-dimensional instantaneous mantle flow induced by subduction. *Geophys. Res. Lett.* 33, L08304 <https://doi.org/10.1029/2005GL025390>.
- Popov, A.A., Sobolev, S.V., 2008. SLIM3D: atool for three-dimensional thermo-mechanical modeling of lithospheric deformation with elasto-visco-plastic rheology. *Phys. Earth Planet. In.* 171, 55–75.
- Popov, A.A., Sobolev, S.V., Zoback, M.D., 2012. Modeling evolution of the San Andreas Fault system in northern and central California. *G-cubed* 13 (8), Q08016. <https://doi.org/10.1029/2012GC004086>.
- Quinteros, J., Sobolev, S.V., Popov, A.A., 2010. Viscosity in transition zone and lower mantle: implications for slab penetration. *Geophys. Res. Lett.* 37, L09307 <https://doi.org/10.1029/2010GL043140>.
- Quinteros, J., Sobolev, S.V., 2012. Constraining kinetics of metastable olivine in the Marianas slab from seismic observations and dynamic models. *Tectonophysics* 526, 48–55.
- Quinteros, J., Sobolev, S.V., 2013. Why has the Nazca plate slowed since the Neogene? *Geology* 41 (1), 31–34.
- Radic, J.P., 2010. Las cuencas cenozoicas y su control en el volcanismo de los Complejos Nevados de Chillán y Copahue-Callaqui (Andes del Sur, 36–39° S). *Andean Geol.* 37 (1), 220–246.
- Ramos, M.E., Folguera, A., Fennell, L.M., Giménez, M., Litvak, V.D., Dzierma, Y., Ramos, V.A., 2014. Tectonic evolution of the North Patagonian Andes from field and gravity data (39–40° S). *J. S. Am. Earth Sci.* 51, 59–75.
- Ramos, M.E., Tobal, J.E., Sagripanti, L., Folguera, A., Orts, D.L., Giménez, M., Ramos, V.A., 2015. The North Patagonian orogenic front and related foreland evolution during the Miocene, analyzed from synorogenic sedimentation and U/Pb dating (~42° S). *J. S. Am. Earth Sci.* 64 (2), 467–485.
- Ramos, V.A., 1999. Plate tectonic setting of the andean cordillera. *Episodes* 22 (3), 183–190.
- Ramos, V.A., Zapata, T., Cristallini, E., Introcaso, A., 2004. The Andean thrust system –latitudinal variations in structural styles and orogenic shortening. In: McClay, K.R. (Ed.), *Thrust Tectonics and Hydrocarbon Systems: AAPG Memoir*, vol. 82, pp. 30–50.
- Ramos, V.A., 2005. Seismic ridge subduction and topography: foreland deformation in the Patagonian Andes. *Tectonophysics* 399, 73–86.
- Ramos, V.A., 2009. Anatomy and global context of the Andes: main geologic features and the Andean orogenic cycle. *Geol. Soc. Am. Mem.* 204, 31–65.
- Ramos, V.A., 2010. The tectonic regime along the Andes: present-day and Mesozoic regimes. *Geol. J.* 45 (1), 2–25.
- Ramos, V.A., Kay, S.M., 1992. Southern Patagonian plateau basalts and deformation: backarc testimony of ridge collisions. *Tectonophysics* 215 (1–3), 261–282.
- Ramos, V.A., Kay, S.M., 2006. Overview of the tectonic evolution of the southern central Andes of Mendoza and Neuquén (35–39° S latitude). *Geol. Soc. Am. Special Pap.* 407, 1–17.
- Ramos, V.A., Kay, S.M., Page, R., Muñizaga, F., 1989. La Ignimbrita Vacas Heladas y el cese del volcanismo en el Valle del Cura, provincia de San Juan. *Rev. Asoc. Geol. Argent.* 44 (1–2), 336–352.
- Rapela, C.W., Spallati, L.A., Merodio, J.C., Aragón, E., 1988. Temporal evolution and spatial variation of early Tertiary volcanism in the Patagonian Andes (40°S–42°30' S). *J. S. Am. Earth Sci.* 1 (1), 75–88.
- Rojas Vera, E.A., Folguera, A., Zamora Valcarce, G., Giménez, M., Ruiz, F., Martínez, P., Ramos, V.A., 2010. Neogene to Quaternary extensional reactivation of a fold and thrust belt: the Agrio belt in the Southern Central Andes and its relation to the Loncopué trough (38–39° S). *Tectonophysics* 492 (1), 279–294.
- Royden, L.H., 1993. The tectonic expression slab pull at continental convergent boundaries. *Tectonics* 12 (2), 303–325.
- Schellart, W.P., 2004. Kinematics of subduction and subduction-induced flow in the upper mantle. *J. Geophys. Res.: Solid Earth* 109, B07401. <https://doi.org/10.1029/2004JB002970>.
- Schellart, W.P., 2008. Overriding plate shortening and extension above subduction zones: a parametric study to explain formation of the Andes Mountains. *Geol. Soc. Am. Bull.* 120 (11–12), 1441–1454. <https://doi.org/10.1130/B26360.1>.
- Schellart, W.P., Moretti, L., 2013. A new driving mechanism for backarc extension and backarc shortening through slab sinking induced toroidal and poloidal mantle flow: results from dynamic subduction models with an overriding plate. *J. Geophys. Res.: Solid Earth* 118 (6), 3221–3248.
- Shockley, B.J., Flynn, J.J., Croft, D.A., Gans, P., Wyss, A.R., 2012. New leontiniid Notoungulata (Mammalia) from Chile and Argentina: comparative anatomy, character analysis, and phylogenetic hypotheses. *Am. Mus. Novit.* 3737, 1–64.
- Silvestro, J., Atencio, M., 2009. La cuenca cenozoica del río Grande y Palauco: edad, evolución y control estructural, faja plegada de Malargüe. *Rev. Asoc. Geol. Argent.* 65 (1), 154–169.
- Sobolev, S.V., Babekyo, A.Y., 2005. What drives orogeny in the Andes? *Geology* 33 (8), 617–620.
- Somoza, R., Zaffarana, C.B., 2008. Mid-Cretaceous polar standstill of South America, motion of the Atlantic hotspots and the birth of the Andean cordillera. *Earth Planet Sci. Lett.* 271, 267–277.
- Somoza, R., Ghidella, M.E., 2005. Convergencia en el margen occidental de América del Sur durante el Cenozoico: subducción de las placas de Nazca, Farallón y Aluk. *Rev. Asoc. Geol. Argent.* 60 (4), 797–809.
- Somoza, R., Ghidella, M.E., 2012. Late Cretaceous to recent plate motions in western South America revisited. *Earth Planet Sci. Lett.* 331, 152–163.
- Streckler, M.R., Alonso, R.N., Bookhagen, B., Carrapa, B., Hille, G.E., Sobel, E.R., Trauth, M.H., 2007. Tectonics and climate of the southern central Andes. *Annu. Rev. Earth Planet. Sci.* 35, 747–787.
- Suárez, M., Emparan, C., 1995. The stratigraphy, geochronology and paleophysiology of a Miocene fresh-water interarc basin, southern Chile. *J. S. Am. Earth Sci.* 8 (1), 17–31.
- van Dinter, Y., Morra, G., Funiciello, F., Faccenna, C., 2010. Role of the overriding plate in the subduction process: insights from numerical models. *Tectonophysics* 484, 74–86.
- van Hunen, J., van den Berg, A.P., Vlaar, N.J., 2002. On the role of subducting oceanic plateaus in the development of shallow flat subduction. *Tectonophysics* 352 (3), 317–333.
- van Hunen, J., van den Berg, A.P., Vlaar, N.J., 2004. Various mechanisms to induce present-day shallow flat subduction and implications for the younger Earth: a numerical parameter study. *Phys. Earth Planet. In.* 146 (1), 179–194.
- Winocur, D.A., Litvak, V.D., Ramos, V.A., 2015. Magmatic and tectonic evolution of the Oligocene Valle del Cura basin, main Andes of Argentina and Chile: evidence for generalized extension. In: Sepúlveda, S.A., Giambiagi, L.B., Moreiras, S.M., Pinto, L., Tunik, M., Hoke, G.D., Fariñas, M. (Eds.), *Geodynamic Processes in the Andes of Central Chile and Argentina*, vol. 399. Geological Society of London, London, pp. 109–130. Special Publications.
- Wyss, A.R., Flynn, J.J., Norell, M.A., Swisher III, C.C., Novacek, M.J., McKenna, M.C., Charrier, R., 1994. Paleogene mammals from the Andes of central Chile: a preliminary taxonomic, biostratigraphic and geochronologic assessment. *Am. Mus. Novit.* 3098, 1–31.